

## Neutrino spin-flip effects in collapsing stars

H. Athar<sup>(1,4)</sup>, J. T. Peltoniemi<sup>(2)</sup>, and A.Yu. Smirnov<sup>(1,3)</sup>

(1)*International Centre for Theoretical Physics, I-34100 Trieste, Italy*

(2)*INFN, Trieste and International School for Advanced Study  
I-34013 Trieste, Italy*

(3)*Institute for Nuclear Research, Russian Academy of Sciences, Moscow, Russia*

(4)*Department of Physics, Quaid-i-Azam University, Islamabad, Pakistan*

### Abstract

We study the spin-flavor transitions of neutrinos,  $\bar{\nu}_e - \nu_\mu$ ,  $\nu_e - \bar{\nu}_\mu$ , etc., in the magnetic fields of a collapsing star. For the neutrino mass squared difference  $\Delta m^2 \sim (10^{-10} - 10) \text{ eV}^2$  the transitions take place in almost isotopically neutral region of the star, where the effective matter density is suppressed up to 3 – 4 orders of magnitude. This suppression is shown to increase the sensitivity of the neutrino bursts studies to the magnetic moment of neutrino,  $\mu$ , by 1.5 – 2 orders of magnitude, and for realistic magnetic field the observable effects may exist for  $\mu \sim (2 - 3) \cdot 10^{-14} \mu_B$  ( $\mu_B$  is the Bohr magneton). In the isotopically neutral region the jumps of the effective potential exist which influence the probabilities of transitions. The experimental signatures of the spin-flavor transitions are discussed. In particular, in the case of direct mass hierarchy, the spin-flip effects result in a variety of modifications of the  $\bar{\nu}_e$ -spectrum. Taking this into account, we estimated the upper bounds on  $\mu B$  from the SN1987A data. In the isotopically neutral region the effects of possible twist of the magnetic field on the way of neutrinos can be important, inducing distortion of the neutrino energy spectra and further increasing the sensitivity to  $\mu B$ . However, if the total rotation angle is restricted by  $\Delta\phi < \pi$ , the absolute change of probabilities is small.

# 1 Introduction

At least 100 neutrino bursts from the gravitational collapses of stars in our Galaxy are already on the way to the Earth<sup>1</sup>. A registration of even one of those by the existing detectors, Kamiokande [2], Baksan [4], LSD [5], and especially, by the new installations: LVD [6] (which is already working), SNO [7] and Superkamiokande [8] (starting to operate in 1996), ICARUS [9] (which is at the prototype stage) will give unique and extremely rich information about features of the gravitational collapse, supernova phenomena and neutrinos themselves. Already SN1987A has given a lot. In general, one will be able to get information on the energy spectra (as a function of time) of  $\nu_e$ ,  $\bar{\nu}_e$ , as well as of neutrinos of the non-electron type:  $\nu_\mu$ ,  $\bar{\nu}_\mu$ ,  $\nu_\tau$ ,  $\bar{\nu}_\tau$ . Certain properties of these spectra do not depend on the model of the star thus opening the possibility to study the characteristics of neutrinos. New experiments are discussed to detect the neutrino bursts from collapses in other nearby galaxies [10].

In this paper we consider a possibility to study effects of the neutrino magnetic moments using the neutrino bursts. In the magnetic fields the neutrinos with magnetic moments undergo spin-precession [11, 12, 13], spin-flavor precession [14] or/and resonant spin-flavor conversion, e.g.  $\nu_{eL} \rightarrow \bar{\nu}_{\mu R}$  [15, 16]. Previously, the applications of these effects to neutrinos from supernova have been considered in [12] (precession) and [15, 17] (resonance conversion).

The spin-flip effects are determined by the product,  $\mu B$ , of the neutrino magnetic moment,  $\mu$ , and the strength of the magnetic field,  $B$ . The discovery of the effects corresponding to values of  $\mu$  near the present upper bound,  $\mu < (1-3) \cdot 10^{-12} \mu_B$  [21] ( $\mu_B$  is the Bohr magneton) will imply rich physics beyond the standard model. From this point of view the studies of the neutrino bursts are of special interest since the magnetic fields in supernova can be as strong as  $(10^{12} - 10^{14})$  Gauss.

It is reasonable to address two questions, keeping in mind that the magnetic field profiles of supernovae are essentially unknown, and vary from the star to star. What are the experimental signatures of the spin-flip effects? And what could be the sensitivity of the neutrino burst studies to the magnetic moments of neutrinos, or more precisely to  $\mu B$ ?

The spin-flip probability may be of the order 1, if

$$\mu \gtrsim \frac{1}{\int dr B(r)}, \quad (1)$$

where the strength of the magnetic field is integrated along neutrino trajectory. Suggesting the field profile

$$B \simeq B_0 \left( \frac{r_0}{r} \right)^k, \quad (2)$$

---

<sup>1</sup>This comes about from the estimation of frequency of the collapses in our Galaxy as 1/30 year [1]

with  $B_0 \sim (10^{12} - 10^{14})$  Gauss,  $k = 2 - 3$ , and  $r_0 \sim 10$  km, where  $r$  is the distance from the center of star, one gets from (1),

$$\mu B_0 \gtrsim \frac{k-1}{r_0} \quad (3)$$

and  $\mu \gtrsim (10^{-15} - 10^{-17})\mu_B$ . (For a constant field a similar bound is  $\mu B \geq (\Delta r_B)^{-1}$ , where  $\Delta r_B$  is the size of region with the magnetic field). These numbers look encouraging, being 3 - 5 orders of magnitude below the present bound.

However, the estimation (1) corresponds to neutrino propagation in vacuum (no matter), where the precession takes place with maximal depth,  $A_P = 1$ . In this case the ‘‘optimal conditions’’ for the spin-flip are realized: the value of  $\mu B$  needed to change the spin-flip probability by a given amount  $\Delta P$  is minimal [22]. The presence of dense matter strongly reduces a sensitivity to  $\mu$ . Forward neutrino scattering (refraction) results in neutrino level splitting:  $\Delta H = V_{SF}$ , where  $V_{SF}$  is the difference of the effective potentials acquired by the left and right handed neutrino components in matter. Typically  $V_{SF} \sim V_0$ , where

$$V_0 \equiv \sqrt{2}G_F n \approx \sqrt{2}G_F \rho / m_N \quad (4)$$

is the total potential,  $G_F$  is the Fermi constant,  $n$  is the nucleon number density,  $\rho$  is the matter density and  $m_N$  is the nucleon mass. The level splitting suppresses the depth of precession [13]:

$$A_P = \frac{(2\mu B)^2}{(2\mu B)^2 + (\Delta H)^2} = \frac{1}{1 + [V_{SF}/2\mu B]^2}, \quad (5)$$

and to have  $A_P \geq \frac{1}{2}$ , one needs

$$\mu B \geq \frac{1}{2}V_{SF}. \quad (6)$$

In dense medium the restriction (6) is much stronger than (3). Indeed, for typical density of the neutrinosphere of the supernova:  $\rho \sim 10^{12}$  g/cm<sup>3</sup> and for  $B \simeq 10^{14}$  Gauss, one gets from (6):  $\mu \geq 10^{-7}\mu_B$ . With increase of distance, the potential  $V_{SF}$  decreases as  $n \propto r^{-3}$ , or quicker, and the restriction (6) relaxes faster than (3). At  $r \gtrsim R_\odot$  it becomes even weaker than (3) (here  $R_\odot \equiv 7 \cdot 10^{10}$  cm is the solar radius).

The suppression of the matter density (i.e., approaching the vacuum condition) results in the increase of the sensitivity to  $\mu$ . This is realized in the case of the resonant spin-flavor conversion [16]. If the left and right handed neutrino components connected by the magnetic moment have different masses,  $m_1, m_2$ , being also of different flavors, the matter effect can be compensated by mass splitting:

$$\Delta H = V_{SF} - \frac{\Delta m^2}{2E} = 0 \quad (7)$$

(*resonance condition*), where  $\Delta m^2 \equiv m_2^2 - m_1^2$ , and  $E$  is the neutrino energy. Now the expression for  $A_P$  becomes

$$A_P = \frac{(2\mu B)^2}{(2\mu B)^2 + \left(V_{SF} - \frac{\Delta m^2}{2E}\right)^2}, \quad (8)$$

and in the resonance (7) one gets  $A_P = 1$ . However, since  $V_{SF}$  changes with distance, the equality  $A_P = 1$  holds only in the resonance point,  $r_R$ . Strong compensation of the matter effects occurs in some layer around  $r_R$  whose size depends on gradient of the potential:  $\dot{V}_{SF} \equiv dV_{SF}/dr$ . Indeed, from (8) one finds that  $A_P \geq \frac{1}{2}$ , if  $\Delta H = \Delta V_{SF} \leq \Delta V_R$ , where

$$\Delta V_R = 2\mu B \quad (9)$$

is the half-width of the resonance layer. The spatial size of the region with  $A_P \geq 1/2$  equals  $2\Delta r_R = 2(\dot{V}_{SF})^{-1}\Delta V_R = 2(\dot{V}_{SF})^{-1}2\mu B$ . Then the strong spin-flip effect implies that  $2\Delta r_R$  is larger than half of the precession length,  $l_p$ :  $2\Delta r_R \gtrsim l_p/2 = \pi/2\mu B$ . Substituting the expression for  $\Delta r_R$  in this inequality one gets

$$\kappa_R \equiv \frac{2(2\mu B)^2}{\pi|\dot{V}_{SF}|} \gtrsim 1. \quad (10)$$

This is the *adiabaticity condition* in the resonance [15, 16], and  $\kappa_R$  is the resonance adiabaticity parameter. (Note that the adiabaticity parameter  $\gamma$  used in [16] is related to that in (10) as  $\kappa_R = 2\gamma/\pi$ ). For large densities the condition (10) is much less restrictive, than (6), allowing for a strong spin-flip effect for smaller values of  $\mu B$ . For example, at  $B = 10^{14}$  Gauss,  $\rho = 10^{12}$  g/cm<sup>3</sup>, and  $V_{SF}/\dot{V}_{SF} \sim r_0 \sim 10$  km, one gets  $\mu > 3 \cdot 10^{-12} \mu_B$ , instead of  $10^{-7} \mu_B$ .

Here we will consider *two new phenomena* which suppress the matter effect and thus, increase the sensitivity of neutrino burst studies to the neutrino magnetic moment. The potential  $V_{SF}$  can be diminished for special nuclear composition of matter. We point out that this is realized in the external region of supernova, where the medium is almost isotopically neutral. Another phenomenon is the magnetic field twist – the change of the direction of the magnetic strength lines on the way of neutrinos. The field twist leads to an additional contribution to the level splitting  $\Delta H$  which can compensate the matter effect.

The experimental signatures of the spin-flavor transitions of supernova neutrinos have been discussed previously in [17]. The influence of the spin-flip on the relation between directional (induced by  $\nu_e e$ -scattering) and isotropic ( $\bar{\nu}_e p$  - interaction) signals was studied. Without consideration of the dynamics of the propagation it was suggested that the probabilities of different transitions are either one or zero. The estimated number of events shows that four cases (1) no transitions, (2) only flavor transitions, (3) only spin-flavor transitions, (4) flavor plus spin-flavor transitions can

be disentangled by new installations (SNO, Superkamiokande). We will consider a more general situation concentrating on the energy dependence of the transitions.

In this paper we study the dynamics of propagation to estimate the values of  $\mu B$  needed for different effects. We consider signatures of the spin-flip transitions related to specific density distribution in the isotopically neutral region and to possible presence of the magnetic field twist. The paper is organized as follows. In Sect. 2, we describe the effective potential in supernova. In Sect. 3 the level crossing schemes for different values of neutrino masses are found and the dynamics of neutrino propagation is considered. In Sect. 4, we study the dependence of the transition probabilities on the magnetic field profile and on the neutrino parameters. Sect. 5 is devoted to the interplay of the spin-flavor and flavor transitions. In Sect. 6 we consider some special effects of neutrino propagation and discuss the possible implications of the results. In particular, we describe the distortion of energy spectra of neutrinos and estimate the sensitivity of the studies of  $\nu$ -bursts to  $\mu B$ . Also, the upper bound on  $(\mu B)$  will be obtained from SN1987A data. In Sect. 7, the effects of the magnetic field twist are considered.

## 2 Isotopically neutral region. Effective potential.

For the spin-flavor transitions, e.g.,  $\nu_{eL} \rightarrow \bar{\nu}_{\mu R}$ ,  $\bar{\nu}_{eR} \rightarrow \nu_{\mu L}$ , the matter effect is described by the potential [15, 16]

$$V_{SF} = \sqrt{2}G_F n(2Y_e - 1) \equiv V_0 (2Y_e - 1), \quad (11)$$

where  $Y_e$  is the number of electrons per nucleon. The value of  $Y_e$  depends on the nuclear composition of the matter. In isotopically neutral medium ( $\#$  protons =  $\#$  neutrons), one has  $Y_e = \frac{1}{2}$ , and according to (11)  $V_{SF} = 0$ . Consequently, the matter effect is determined by the deviation from the isotopical neutrality.

For the flavor conversion the potential is proportional to the electron density:

$$V_F \simeq \sqrt{2}G_F n Y_e = V_0 Y_e . \quad (12)$$

Evidently, there is no suppression of  $V_F$  in the isotopically neutral medium;  $V_F$  is suppressed in the central strongly neutronized region of the star.

### 2.1 Isotopically neutral region

The progenitor of the type II supernova has the ‘‘onion’’ structure. Below the hydrogen envelope the layers follow which consist mainly of the isotopically neutral nuclei:  ${}^4\text{He}$ ,  ${}^{12}\text{C}$ ,  ${}^{16}\text{O}$ ,  ${}^{28}\text{Si}$ ,  ${}^{32}\text{S}$ . Thus the region between the hydrogen envelope and the core, where elements of iron peak

dominate, is almost isotopically neutral. The deviation from the neutrality is stipulated by small abundances,  $\xi_i$ , of the elements with small excess of neutrons,  $i = {}^{22}\text{Ne}, {}^{23}\text{Na}, {}^{25}\text{Mg}, {}^{56}\text{Fe}$  [23, 24]. It can be written as

$$(1 - 2Y_e) \approx \sum_i \xi_i \cdot \left(1 - \frac{2Z_i}{A_i}\right), \quad (13)$$

where  $Z_i$  and  $A_i$  are the electric charge and the atomic number of nuclei “ $i$ ”, correspondingly. Typically, one gets  $\sum_i \xi_i \leq 10^{-2}$  and  $(1 - \frac{2Z}{A}) \leq 10^{-1}$ , and therefore, according to (13):  $(1 - 2Y_e) \leq 10^{-3}$ . The value of  $(2Y_e - 1)$  equals

$$(2Y_e - 1) = \begin{cases} 0.6 - 0.7 & \text{hydrogen envelope} \\ -(10^{-4} - 10^{-3}) & \text{isotopically neutral region} \\ -(0.2 - 0.4) & \text{central regions of star} \end{cases} \quad (14)$$

Consequently, in the isotopically neutral region the potential  $V_{SF}$  is suppressed by more than 3 orders of magnitude with respect to the total potential  $V_0$  (fig.1). We calculated the potentials using the model of the progenitor with mass  $15M_\odot$  (where  $M_\odot$  is the solar mass) [23]. Two remarks are in order. For  $r < R_\odot$  the spatial distributions of the total density, are very similar (up to factor 2) for stars in a wide range of masses:  $M = (12 - 35)M_\odot$ . The profiles may differ appreciably in the external low density regions which are unessential for our consideration. The collapse of the core and the propagation of the shock wave change both the density profile and the nuclear composition of medium. However, during the neutrino burst (0 - 10 seconds after the core bounce) the shock wave can reach the distance  $\sim$  several 1000 km at most. Therefore most part of the isotopically neutral region turns out to be undisturbed and one can use the profile of the progenitor.

Strong convection effects in the inner and intermediate parts of the star, if exist, may result in an injection of the elements in the iron peak into outer layers, thus diminishing the degree of the isotopical neutrality.

## 2.2 Properties of the effective potential

According to (14) and Fig. 1, the effective potential  $V_{SF}$  has the following features: It is positive and of the order  $V_0$  in the H-envelope;  $V_{SF}$  decreases quickly and changes the sign in the border between the hydrogen envelope and the  ${}^4\text{He}$ -layer ( $r \sim R_\odot$ );  $V_{SF}$  is negative and suppressed by 3 - 4 orders of magnitude in comparison with  $V_0$  in the isotopically neutral region;  $V_{SF}$  quickly increases in the inner edge of the isotopically neutral region ( $r \sim 10^{-3}R_\odot$ ), and becomes again of the order  $V_0$  in the central part of the star. In the isotopically neutral region the jumps of the effective potential  $V_{SF}$  (not  $V_0$ !) exist which are related to the change of the nuclear composition in the layers of local nuclear ignition. The jump may be as large as an order of magnitude.

The isotopically neutral region spreads from  $10^{-3}R_\odot$  to  $\approx R_\odot$  (Fig. 1). Here the potential changes from  $V_{SF} = (10^{-9} - 10^{-8})$  eV to zero:  $V_{SF} \rightarrow 0$ , when  $r \rightarrow (0.8 - 1)R_\odot$ . Below  $10^{-17}$  eV, however,  $V_{SF}(r)$  decreases so quickly that no matter effects are induced. The detectable energy range of the neutrinos from the gravitational collapse is (5 – 50) MeV. Consequently, in the isotopically neutral region the resonance condition (7) is fulfilled for  $\Delta m^2 \sim (10^{-10} - 0.1)$  eV<sup>2</sup>. This covers the range of  $\Delta m^2$  interesting from the point of view of the solar and the atmospheric neutrino problems. For the cosmologically interesting values,  $\Delta m^2 \sim (4 - 50)$  eV<sup>2</sup>, the resonance is at the inner part of the isotopically neutral region, where the potential is still suppressed by factor  $1/30 - 1/100$ .

Let us stress that the suppression of the effective density takes place for the spin-flavor conversion only, i.e. when both neutrino components are active. In the case of the spin-flip into sterile neutrino  $\nu_e \rightarrow \bar{\nu}_s$ , the effective potential equals  $V_s = \frac{V_0}{2}(3Y_e - 1)$ , and in the isotopically neutral region one has  $V_s = \frac{V_0}{4}$ . The potential  $V_s$  is suppressed in strongly neutronized central part of star, where  $Y_e \approx \frac{1}{3}$  [18, 19].

### 3 The dynamics of the neutrino transitions

#### 3.1 Level crossing scheme

We will consider the system of three massive neutrinos with transition magnetic moments and vacuum mixing (see [30] for details). For definiteness we assume the direct mass hierarchy:  $m_1 \ll m_2 \ll m_3$  and the smallness of flavor mixing. The energies of the flavor levels (the diagonal elements of the effective Hamiltonian),  $H_\alpha$ , ( $\alpha = \nu_e, \bar{\nu}_e, \nu_\mu, \bar{\nu}_\mu, \nu_\tau, \bar{\nu}_\tau$ ), can be written as

$$\begin{aligned} H_e &\equiv 0, \\ H_{\bar{e}} &\equiv -V_0 (3Y_e - 1) - \dot{\phi}, \\ H_\mu &\equiv \cos 2\theta \frac{\Delta m^2}{4E} - V_0 Y_e, \\ H_{\bar{\mu}} &\equiv \cos 2\theta \frac{\Delta m^2}{4E} - V_0 (2Y_e - 1) - \dot{\phi}. \end{aligned} \tag{15}$$

Here  $\theta$  is the  $e$ - $\mu$ -mixing angle in vacuum. The  $\nu_\tau$  energy levels,  $H_\tau, H_{\bar{\tau}}$ , can be obtained from  $H_\mu, H_{\bar{\mu}}$  by substituting  $\theta \rightarrow \theta_\tau$  and  $\Delta m^2 \rightarrow \Delta m_{31}^2$ . The angle  $\phi(t)$  ( $\dot{\phi} \equiv d\phi/dr$ ) defines the direction of the magnetic field in the transverse plane. In (15) for later convenience, we have subtracted from all elements the energy  $H_e$  to make the first diagonal element of the Hamiltonian (i.e.,  $H_e$ ) equal to zero. (This is equivalent to the renormalisation of all wave functions by the same factor which does not change the probabilities). The qualitative dependence of the energy levels  $H_\alpha$  on distance  $r$  for  $\dot{\phi} = 0$  and for different values of  $\Delta m^2/2E$  is shown in Fig. 2. The resonance (level crossing) conditions read as  $H_\alpha = H_\beta$  ( $\alpha \neq \beta$ ).

The peculiar behavior of the effective potential  $V_{SF}$  in the isotopically neutral region stipulates a number of features in the level crossing scheme. With increase of  $\Delta m^2$  one gets the following changes. (The levels for  $\nu_e$  and  $\bar{\nu}_e$  are fixed, whereas  $\nu_\mu$ - and  $\bar{\nu}_\mu$ -levels go up).

For  $\Delta m^2 \lesssim 10^{-10} \text{eV}^2$  ( $E \sim 20 \text{ MeV}$ ) the mass splitting can be neglected. Two crossings of the levels which correspond to the spin-flavor conversions  $\nu_e \rightarrow \bar{\nu}_\mu$  and  $\bar{\nu}_e \rightarrow \nu_\mu$  occur practically at the same point, where  $(2Y_e - 1) \simeq 0$  ( $r \simeq 0.8R_\odot$ ), i.e. on the border between the H-envelope and  ${}^4\text{He}$ -layer. The crossings are stipulated by change of nuclear composition of the star (Fig. 2a).

For  $\Delta m^2 \gtrsim 10^{-10} \text{eV}^2$  the spin-flavor resonances,  $\nu_e - \bar{\nu}_\mu$  and  $\bar{\nu}_e - \nu_\mu$ , are spatially splitted. With increase of  $\Delta m^2$  the  $\bar{\nu}_e - \nu_\mu$  resonance shifts to the center of star, whereas  $\nu_e - \bar{\nu}_\mu$  does to the surface. Moreover, second resonance of  $(\bar{\nu}_e - \nu_\mu)$ -type appears in the outer layers. When  $\Delta m^2$  increases these same resonances approach each other, and at  $\Delta m^2 \sim 3 \cdot 10^{-8} \text{eV}^2$  merge (a “touching” point of  $\nu_e$ - and  $\bar{\nu}_\mu$ -levels) (Fig. 2b).

For  $\Delta m^2 \gtrsim 3 \cdot 10^{-8} \text{eV}^2$ , there is only one spin-flavor resonance,  $\bar{\nu}_e - \nu_\mu$ . The flavor resonance  $\nu_e - \nu_\mu$  lies closer to the surface. When  $\Delta m^2$  increases both these resonances shift to the center (Fig. 2c).

The  $\nu_\tau$ -level can cross  $\nu_e$ - and  $\bar{\nu}_e$ -levels in the isotopically neutral region. Moreover, for cosmologically interesting values of  $\Delta m_{13}^2$  the  $\nu_\tau$ -resonances are in inner edge of this region. They can also be in the central part of the star.

### 3.2 Adiabaticity conditions

In the isotopically neutral region the effective potentials for the flavor conversion and the spin-flavor conversion differ by 3 – 4 orders of magnitude. Therefore, the flavor and spin-flavor resonances are strongly separated in space, in contrast with the case of usual medium. Consequently, one can consider these crossings independently, reducing the task to two neutrino tasks.

If  $\theta$  is small the flavor transition is essentially a local resonance phenomenon. It takes place at  $r_R$  determined from (15):  $H_\mu(r_R) = 0$ . Therefore, the effect depends on the local properties of the density distribution in resonance:  $V_F(r_R) = V_0 Y_e(r)$  and  $H_F \equiv V_F / \dot{V}_F|_{r_R}$ . The flavor adiabaticity reads

$$\kappa_R^F \equiv \frac{H_F}{\pi} \cdot \frac{\Delta m^2}{E} \cdot \frac{\sin^2 2\theta}{\cos 2\theta} > 1. \quad (16)$$

(This corresponds to the situation when at least half of the oscillation length, is obtained in the resonance layer, in the direct analogy with the definition of the adiabaticity parameter for the spin-flip conversion (10)). Using the potential  $V_F \sim V_0$  (fig. 1), we find that for neutrinos with  $E \sim 20 \text{ MeV}$  and  $\Delta m^2 = 10^{-6}, 10^{-5}, 10^{-4}$  and  $10^{-2} \text{eV}^2$ , the resonance is situated at  $r = 0.7R_\odot, 0.5R_\odot, 0.17R_\odot, 0.03R_\odot$ , correspondingly, and the condition (16) is satisfied for  $\sin^2 2\theta > 0.5, 0.06, 0.02$ ,



$10^{-3}$ .

In contrast, the spin-flip effects can be nonlocal even in case of variable density. Indeed, the helicity mixing angle,  $\theta_B$ , which determines the mixing between the left and the right components (in ultrarelativistic case) is

$$\tan 2\theta_B = \frac{2\mu B}{V_{SF} - \frac{\Delta m^2}{2E}}. \quad (17)$$

(In medium with constant parameters  $\theta_B$  determines the depth of precession, when the initial state has a definite chirality:  $A_P = \sin^2 2\theta_B$ ). Since in general the field strength depends on distance, the angle  $\theta_B$  can be large enough in a wide spatial region provided  $\mu B \sim V_{SF} \gg \Delta m^2/2E$ . For large  $B$  the spin-flip effect may not be localized in the resonance layer, and moreover, the resonance itself may not be local [30].

The rapidity of the  $\theta_B$  change on the way of neutrino,  $\dot{\theta}_B \equiv d\theta_B/dr$ , determines the adiabaticity condition for spin-flip:

$$\pi\dot{\theta}_B \lesssim \Delta H = \sqrt{(2\mu B)^2 + \left(V_{SF} - \frac{\Delta m^2}{2E}\right)^2}.$$

The adiabaticity parameter can be written as

$$\kappa \equiv \frac{\Delta H}{\pi\dot{\theta}_B} = \frac{(V^2 + (2\mu B)^2)^{3/2}}{\pi(\mu\dot{B}V - \dot{V}\mu B)}, \quad (18)$$

here  $V \equiv V_{SF} - \Delta m^2/2E$ . In resonance,  $V = 0$  or  $V_{SF} \cong \Delta m^2/2E$ , the expression (18) reduces to (10). Beyond the resonance  $\kappa$  depends on the magnetic field change. In the extreme cases one has

$$\kappa \approx \begin{cases} \kappa_R \left(\frac{V_{SF}}{\mu B}\right)^3, & V_{SF} \gg \Delta m^2/2E \\ \kappa_R \left(\frac{\Delta m^2/E}{\mu B}\right)^2 \left(\frac{\dot{V}_{SF}}{\mu \dot{B}}\right), & V_{SF} \ll \Delta m^2/2E \end{cases}, \quad (19)$$

where  $\kappa_R$  is the resonance adiabatic parameter for a given point (10). According to (19) the adiabaticity condition is strongly relaxed, if  $V_{SF} \gg \mu B$  above the resonance, and if  $\Delta m^2/2E \gg \mu B$  below the resonance. For the density and the field profiles under consideration these inequalities are fulfilled, so that the adiabaticity is the most crucial in the resonance.

If the initial and final mixings are small:  $\theta_B^i \approx \pi/2$  and  $\theta_B^f \approx 0$  and the level crossing is local, one can estimate the survival probability using the Landau-Zener formula:

$$P \approx P_{LZ} = e^{-\frac{\pi^2}{4}\kappa_R} = e^{-\frac{\pi^2}{4}\left(\frac{B}{B_A}\right)^2}, \quad (20)$$

where  $B_A^2 \equiv \pi\dot{V}/8\mu^2$  (see (10)). At the adiabatic condition,  $B = B_A$ , one gets  $P_{LZ} = 0.085$ . The probability increases quickly with decrease of the field:  $P_{LZ} = 0.3, 0.54, 0.8$ , when  $B/B_A = 0.7, 0.5, 0.3$  correspondingly (see Fig. 3). An appreciable effect could be for  $P_{LZ} = 0.8$ , when the magnetic field is about 3 times smaller than the adiabatic value.

### 3.3 The precession and the adiabaticity bounds

The propagation of neutrinos with magnetic moment in the magnetic field and matter is an interplay of two processes: the precession and the resonance spin conversion. A relation between them is determined largely by density distribution. Let us define the *precession bound* for the product  $(\mu B)_P$  as

$$\mu B_P = \frac{1}{2} V_{SF}. \quad (21)$$

At  $(\mu B) = (\mu B)_P$ , the precession may have the depth  $A_P = 1/2$  (see (6)); for  $(\mu B) \ll (\mu B)_P$  the precession effects can be neglected. Let us also introduce the *adiabaticity bound*  $(\mu B)_A$  using the adiabaticity condition (10):

$$(\mu B)_A = \sqrt{\frac{\pi \dot{V}_{SF}}{8}} \approx \sqrt{\frac{\pi}{8 H_{SF}}} V_{SF}^{1/2}, \quad (22)$$

where  $H_{SF} \equiv [dV_{SF}/dx]^{-1} V_{SF}$  is the typical scale of the potential change. For  $(\mu B) > (\mu B)_A$  the level crossing is adiabatic. Comparing (21) and (22) one finds that for fixed  $H_{SF}$  the precession bound increases with  $V_{SF}$  faster than the adiabaticity bound. Consequently, for large  $V_{SF}$ , the inequality  $(\mu B)_P \gg (\mu B)_A$  holds and the conversion dominates over precession. The suppression of  $V_{SF}$  makes the precession effect more profound. If the potential changes as  $V_{SF} \propto r^{-3}$ , one gets

$$(\mu B)_A \propto \frac{1}{r^2}, \quad (\mu B)_P \propto \frac{1}{r^3}. \quad (23)$$

Clearly,  $(\mu B)_P < (\mu B)_A$  in the hydrogen envelope, and  $(\mu B)_P > (\mu B)_A$  in the center of star. The adiabatic conversion dominates in the inner parts, whereas the precession may dominate in the external layers of star (Fig. 3). In the isotopically neutral region one has  $(\mu B)_P \sim (\mu B)_A$ , i.e., both processes may be essential (see Sect. 4). In fact, the condition (21) is not sufficient for a strong spin-precession effect. The spatial size of the region where (21) is fulfilled,  $\Delta r$ , should be large enough, so that the inequality (1) or  $\Delta r \gtrsim 1/\mu B$  is satisfied. For  $r > 0.3 R_\odot$  the latter bound is even stronger than (21). Instead of  $\mu B$ , in further discussion we will give the estimations of the magnetic fields at  $\mu = 10^{-12} \mu_B$ . Rescaling to other values of  $\mu$  is obvious.

The adiabaticity and the precession bounds determined by the density distribution should be compared with the magnetic field profile of star. In fig. 3, we depict the profile (2) with  $k = 2$  and  $B_0 = 1.5 \cdot 10^{13}$  Gauss. The strength of this field is practically everywhere below both the adiabatic,  $B_A$ , and the precession,  $B_P$ , bounds ( $\mu = 10^{-12} \mu_B$ ) which means that spin-flip effects are rather weak. The effects of the global field (2) may be strong, when  $B_0 \geq 10^{14}$  Gauss. However, for  $k = 3$  even extremely large central field,  $B_0 \sim 10^{17}$  Gauss, corresponds to very weak magnetic field in the isotopically neutral region. Local mechanisms of the magnetic fields generation due to possible

convection and differential rotation may produce the local field being much larger than the global field, as in the case of the Sun.

### 3.4 Effects of jumps of the potential

The electron density number  $n(2Y_e - 1)$ , and consequently, the effective potential  $V_{SF}$  change quickly in the ignition layers, so that for reasonable values of  $\mu B$  the adiabaticity is broken. This feature is reflected by peaks in the adiabaticity bound (fig. 3). To a good approximation one can consider these changes as sudden jumps of the potential,  $\Delta V_j \equiv V_{\max} - V_{\min}$ , at fixed points  $r_j$ . The effect of jump reduces to jump-like change of the helicity mixing angle  $\theta_B$ .

The jumps distort the energy dependence of probabilities. The position of the energy interval affected by the jump is related via the resonance condition to the values of  $V_{\min}$  and  $V_{\max}$ . The character of distortion depends on the magnitude of jump,  $\Delta V_{SF}$ , as compared with the energy width of the resonance layer  $\Delta V_R$  ( $\Delta V_R = 2\mu B$ ). (See a similar consideration for the flavor case in [25]). If  $\Delta V_j \leq \Delta V_R$ , the jump leads to the peak of the survival probability with width,  $\Delta E$ , determined by the width of the resonance layer:  $\Delta E/E \sim 2\mu B/V_{SF}(r_j)$  [25]. The height of the peak is given by the ratio:

$$\Delta P \sim \left( \frac{\Delta V_j}{\Delta V_R} \right)^2 = \left( \frac{\Delta V_j}{2\mu B} \right)^2 .$$

For  $2\mu B \gg \Delta V_j$  the jump effect is smoothed: since the size of the resonance region is large, the width of peak is also large, but its height turns out to be suppressed.

If  $\Delta V_j \geq 2\Delta V_R \approx \mu B$ , the height of the peak is of the order 1, and the width is fixed by the size of jump:

$$\frac{\Delta E}{E} \sim \frac{\Delta V_j}{V_{SF}} .$$

For  $\Delta V_{SF} \gg \Delta V_R$ , the jump suppresses the transition in the interval with minimal and maximal energies determined by  $V_{\max}$  and  $V_{\min}$ .

The most profound effect appears, when without jump the adiabaticity is fulfilled and the transition is practically complete. If the width of the resonance is small ( $2\mu B < V_{SF}$ ) and if  $\Delta V_j \sim \Delta V_R$ , the jump induces a thin peak of the survival probability. Such conditions can be fulfilled in the inner part of the isotopically neutral region.

Note that in the considered model of the star there are two big jumps of the potential ( $\Delta V_j/V_{SF} \sim 10$ ) at  $r = 7 \cdot 10^{-2} R_\odot$  and  $r = 0.3 R_\odot$  (fig.1). Also small jumps ( $\Delta V_j/V_{SF} \lesssim 1$ ) exist.

The elements of the dynamics presented here allow to understand all features of the evolution of the neutrino state.

## 4 Neutrino propagation in isotopically neutral region

Let us consider for definiteness the spin-flavor transitions  $\bar{\nu}_e - \nu_\mu$  and  $\nu_e - \bar{\nu}_\mu$ . If  $\Delta m^2 \leq 0.1 \text{ eV}^2$  the level crossing takes place in the isotopically neutral region. For realistic magnetic fields (profile (2) with  $B_0 \ll 10^{17}$  Gauss) the effect of  $\bar{\nu}_e - \nu_\mu$  mixing can be neglected in the inner part of the star. Therefore, the spin-flavor evolution of the neutrino state starts from the inner part of the isotopically neutral region  $r_i \sim 10^{-3} R_\odot$ . At  $r_i$  the states coincide practically with pure helicity/ flavor states. Flavor conversion, if efficient, can be taken into account as further independent transformation (sect. 5). Also the transitions which involve  $\nu_\tau$  can be considered separately.

### 4.1 Spin-flip effects in global magnetic field

We use the profile (2) with  $k = 2$  and take different values of  $B_0$ . For  $B_0 \lesssim 2 \cdot 10^{13}$  Gauss the magnetic field strength is below the precession bound ( $\mu = 10^{-12} \mu_B$ ) in the isotopically neutral region. Consequently, the depth of the precession is suppressed, and the transition has a local resonance character (fig. 4). The transition occurs only in the resonance region whose width is determined by  $\Delta V_R / V_{SF} = 2\mu B / V_{SF}$ . The efficiency of the transition depends on  $\kappa_R$ . The strongest effect takes place for the energies (over  $\Delta m^2$ ),  $E / \Delta m^2$ , which correspond to the weakest violation of the resonance adiabaticity ( $B(r)$  is closer to the adiabaticity bound (fig. 3, 4)). With the increase of  $B_0$  the  $E / \Delta m^2$  range of strong conversion expands (fig. 5).

If  $B_0 \gtrsim 5 \cdot 10^{13}$  Gauss, the field profile is above both the precession and the adiabatic bounds, and the conversion becomes essentially nonlocal (fig. 4). For  $E / \Delta m^2 > 10^3 \text{ MeV/eV}^2$  initial mixing is still very small:  $\theta_B \approx \pi/2$ ,  $\sin^2 2\theta_B \approx 0$ . Therefore, the neutrino state coincides with one of the eigenstates in medium. Since the adiabaticity is fulfilled, the survival probability is uniquely determined by the helicity mixing angle:  $P(\nu_e \rightarrow \nu_e) \approx \cos^2 \theta_B$ . The precession effects are very small (fig. 4). Before the resonance the angle is determined from  $\tan 2\theta_B \approx \mu B(r) / V_{SF}(r)$ . The mixing increases, when the neutrino enters the isotopically neutral region, and if  $\mu B \gg V_{SF}$  the probability approaches  $P \sim 1/2$  (fig. 4). After the resonance layer the angle diminishes quickly:  $\tan 2\theta_B \sim 2\mu B / (\Delta m^2 / 2E)$ , since the magnetic field decreases with distance, whereas the splitting approaches the asymptotic value  $\Delta m^2 / E$ . Correspondingly, the probability goes to zero and one has almost complete spin-flip with  $P(\nu_e \rightarrow \nu_e) \approx 0$  (fig. 4).

For large  $E / \Delta m^2$  the resonance is in the external layers of the star, where the adiabaticity is broken. The final survival probability increases with  $E / \Delta m^2$ , approaching the value of probability before the resonance. As the result one gets  $P \gtrsim 1/2$ . At very large  $E / \Delta m^2$  mass splitting becomes unessential and the dependence of probability on  $E / \Delta m^2$  disappears.

The bump in the survival probability  $P(E)$  in the energy interval  $E / \Delta m^2 = (10^7 - 10^8)$

MeV/eV<sup>2</sup> (fig. 5) is due to a density jump at  $r = (0.1 - 0.5)R_\odot$  (fig. 4 a). For very large  $\mu B$  the effect of jump is suppressed according to the discussion in sect. 3.4.

## 4.2 Spin-flip in local magnetic field

Let us suppose that a strong magnetic field exists in some spatial region  $\Delta r$  between  $r_1$  and  $r_2$ , so that the transitions take place in  $\Delta r$  only. For simplicity we consider a constant magnetic field  $B_c$ . If  $\mu B$  is below the precession bound, the conversion occurs in the resonance layer, and the transition probability is determined by  $\kappa_R$ . The effect is appreciable in the energy interval determined via the resonance condition by the maximal and minimal values of the potential in the layer with magnetic field (fig. 6). When the adiabaticity is broken, the maximal effect corresponds to the resonance in the central part of the region with the magnetic field. In this case there is no averaging over the precession phase and smooth dependence of the probability on energy can be modulated. The energy dependence can be distorted also by jumps of the potential.

If the field is strong enough and the adiabaticity condition is fulfilled, the average probability follows the change of helicity mixing angle  $\theta_B(r)$  (17). The survival probability, as a function of  $E/\Delta m^2$  is determined by the adiabatic formula:

$$P_{\nu_e \rightarrow \nu_e} = \frac{1}{2} \left( 1 + \cos 2\theta_B^i \cos 2\theta_B^f \right) + \frac{1}{2} \sin 2\theta_B^i \sin 2\theta_B^f \cos \Phi, \quad (24)$$

where  $\Phi$  is the precession phase:

$$\Phi = \int_{r_1}^{r_2} dr \sqrt{(2\mu B)^2 + (V_{SF} - \Delta m^2/2E)^2}. \quad (25)$$

Here  $\theta_B^i$  and  $\theta_B^f$  are the values of the mixing angle (17) at  $r_1$  and  $r_2$ . For  $\mu B \gg V_{SF}$ , the influence of matter is small and the survival probability is large for  $E/\Delta m^2 > 1/(\mu B)$ . If  $E/\Delta m^2 \gg 1/(\mu B)$  the precession has maximal depth (fig. 6).

## 4.3 On the energy dependence of probability

The survival probability as function of the neutrino energy has some common features for different magnetic field profiles. There are two characteristic energies:  $(E/\Delta m^2)_{\min}$  and  $(E/\Delta m^2)_{\max}$ . The former,  $(E/\Delta m^2)_{\min}$ , is determined by the adiabaticity violation in the inner part of the isotopically neutral region, or in the inner part of the region with magnetic field (in the case of the local field). The latter,  $(E/\Delta m^2)_{\max}$ , is fixed in such a way that for  $E > E_{\max}$  the effect of mass splitting can be neglected. For the local field  $(E/\Delta m^2)_{\max}$  is determined by the potential at the outer edge of the region with magnetic field. In the case of global field one has  $(E/\Delta m^2)_{\max} \approx 10^{-10}$  eV<sup>2</sup> which

follows from the adiabaticity violation due to a fast decrease of  $\mu B$  or  $V_{SF}$  at the border of the isotopically neutral region (fig. 3).

The energies  $(E/\Delta m^2)_{\max}$  and  $(E/\Delta m^2)_{\min}$  divide the whole energy interval into three parts.

1). Region of matter/vacuum suppression of the spin-flip:  $E/\Delta m^2 < (E/\Delta m^2)_{\min}$ . For neutrinos with such energies before the resonance layer the precession amplitude is strongly suppressed by matter effect. There is no appreciable conversion in the resonance region, since the adiabaticity is strongly broken; after the resonance the amplitude is suppressed by vacuum splitting:  $A_P \sim (\mu B)/(\Delta m^2/E)$ . As a result, the probability of spin-flip is small.

2). Resonance region:  $(E/\Delta m^2)_{\max} < E/\Delta m^2 < (E/\Delta m^2)_{\min}$ . The resonance is in the isotopically neutral region. If the adiabaticity is unbroken or weakly broken, the survival probability is small. Smooth energy dependence of  $P$  due to conversion can be modulated by the effect of density jumps, as well as by the precession effect, if e.g. the initial mixing angle is not small.

3). Precession (asymptotic) region:  $E/\Delta m^2 > (E/\Delta m^2)_{\max}$ . Here the mass splitting  $(\Delta m^2/E)$  can be neglected, and therefore the spin-flip probability does not depend on energy. The spin-flip is due to precession and possible adiabatic (non-resonance) conversion.

If the layers with magnetic field are in the inner part of the isotopically neutral region, the resonance effects can be more profound. Here the adiabaticity condition is fulfilled, even when the width of the resonance is small,  $2\mu B/V_{SF} < 1$ . For the external layers with small density the adiabaticity holds for  $2\mu B/V_{SF} > 1$  only, i.e. when the width of resonance is large.

## 5 Spin-flip and other transitions

### 5.1 Spin-flip and flavor conversion

Let us consider the effects of the flavor conversion  $\nu_e - \nu_\mu$  in addition to the spin-flip. In the isotopically neutral region the positions of the spin-flavor resonance,  $r_s$ , and the flavor resonance,  $r_f$ , are strongly separated in space:  $r_s \ll r_f$ . If the flavor mixing as well as the magnetic field strength are sufficiently small, both flavor and spin-flavor transitions are local. The crossings of flavor and spin-flavor resonance layers are independent, and the total transition probability is the product of the flavor and the spin-flavor probabilities.

Three neutrino states,  $(\nu_e, \bar{\nu}_e, \nu_\mu)$ , are involved in the transitions. Correspondingly, one can introduce  $3 \times 3$  matrix of probabilities  $S$  which relates the original,  $F^0 = (F^0(\nu_e), F^0(\bar{\nu}_e), F^0(\nu_\mu))$ , and the final,  $F = (F(\nu_e), F(\bar{\nu}_e), F(\nu_\mu))$ , fluxes:

$$F = SF^0. \quad (26)$$

Let  $r'$  be some point between the two resonances:  $r_s \ll r' \ll r_f$ . Then in the region  $r < r'$  the matrix  $S$  depends only on the spin-flavor transition probability,  $P_s(\bar{\nu}_e - \nu_\mu)$ :  $S = S_s(P_s)$ . (Evidently,  $(1 - P_s)$  coincides with the survival probability calculated in the sect. 4). In the region  $r > r'$  the matrix  $S$  depends on the flavor transition probability,  $P_f(\nu_e - \nu_\mu)$  transition:  $S = S_f(P_f)$ . The total matrix is the product  $S = S_s(P_s) \times S_f(P_f)$ :

$$S = \begin{pmatrix} (1 - P_f) & P_f P_s & P_f(1 - P_s) \\ 0 & (1 - P_s) & P_s \\ P_f & (1 - P_f)P_s & (1 - P_f)(1 - P_s) \end{pmatrix}. \quad (27)$$

Let us consider the dependence of  $S$  on energy. If the flavor mixing is small (say  $\sin^2 2\theta < 0.01$ ), and the magnetic field is situated in the external part of the star, the energy regions of the strong flavor transition and the strong spin-flip effect do not overlap. The neutrinos of high energies flip the helicity, whereas low energy neutrinos undergo the flavor transition. The overlap of the resonance regions for the spin-flip and the flavor conversion takes place for sufficiently large mixing angles or/and if there is a strong enough magnetic field in the inner part of star:  $r < 0.3R_\odot$  (Fig. 7). In the overlapping energy region the probabilities  $P_s$  and  $P_f$  differ from zero and the electron neutrinos undergo a double transition:  $\bar{\nu}_e \rightarrow \nu_\mu \rightarrow \nu_e$  (fig. 7).

## 5.2 Effects of tau neutrino

Inclusion of  $\nu_\tau$  adds two new level crossings: the flavor,  $(\nu_e - \nu_\tau)$ , and spin-flavor,  $(\bar{\nu}_e - \nu_\tau)$  ones (fig. 2). Other crossings involving  $\nu_\mu$  and  $\nu_\tau$  do not give observable effects. Due to the assumed mass hierarchy the transitions with  $\nu_\tau$  (the inner region of the star) can be considered independently from the transitions involving  $\nu_\mu$  (outer part). Consequently, the total transition matrix is the product of the transition matrices in the inner and the outer regions.

Three states,  $\nu_e, \bar{\nu}_e, \nu_\tau$ , are transformed in the inner part (fig. 2). For monotonously decreasing density, the order of resonances is the same as before: first – spin-flavor and then flavor one. If the  $\nu_\tau$  resonances are enough separated, the transition matrix can be found from that in (27) by substitution  $P_f \rightarrow P'_f$  and  $P_s \rightarrow P'_s$ , where  $P'_f$  and  $P'_s$  are the  $2\nu$ -probabilities of flavor and spin-flavor transitions in the inner region. (In fact one should consider  $4 \times 4$  transition matrices in the  $(\nu_e, \bar{\nu}_e, \nu_\mu, \nu_\tau)$ -basis in the inner and the outer parts and find their product.) The effects due to the  $\nu_\tau$ -resonances can be taken into account as the initial conditions,  $F^i$ , for the fluxes at the border with the outer region. Using the matrix (27) with substitution mentioned above we get

$$\begin{aligned} F(\nu_e)^i &= (1 - P'_f)F^0(\nu_e) + P'_f P'_s F^0(\bar{\nu}_e) + P'_f(1 - P'_s)F^0(\nu_\tau), \\ F(\bar{\nu}_e)^i &= (1 - P'_s)F^0(\bar{\nu}_e) + P'_s F^0(\nu_\tau), \\ F(\nu_\mu)^i &= F^0(\nu_\mu). \end{aligned} \quad (28)$$

Further on we will concentrate on the cosmologically interesting values  $m_3 \sim (2 - 7)$  eV. This corresponds to  $\Delta m^2 = (4 - 50)$  eV<sup>2</sup>, so that for  $E \sim 20$  MeV the resonances are in the inner part of the isotopically neutral region:  $r \sim (1 - 2) \cdot 10^{-3} R_\odot$ . Here the total density is  $(0.3 - 3) \cdot 10^8$  g/cm<sup>3</sup> and  $(1 - 2Y_e) \sim (2 - 4) \cdot 10^{-2}$ . According to fig. 3, the precession bound equals  $(10^{13} - 3 \cdot 10^{15})$  Gauss, and the adiabaticity bound is  $(0.5 - 2) \cdot 10^{11}$  Gauss. Thus an appreciable spin-flip transition implies very large magnetic field:  $B > 10^{10}$  Gauss. In contrast, the flavor transitions can be efficient even for very small mixing angles:  $\sin^2 2\theta > 10^{-6}$ . For  $\Delta m^2$  under consideration the spin-flip effects may be more probable below the isotopically neutral region.

### 5.3 Transitions in the central region of the star

The collapse and the shock wave propagation lead to strong time dependence of the density profile in the central region of the star. Moreover, the profile may be non-monotonous. With approaching the center of star the total matter density may first diminish from  $10^8$  g/cm<sup>3</sup> to  $(10^6 - 10^7)$  g/cm<sup>3</sup> at  $r \sim 100$  km, and then rapidly increase at the surface of the protoneutron star,  $r < (20 - 30)$  km. Moreover, in the central part the neutrino-neutrino scattering should be taken into account [34]. Due to the non-monotonous behavior of  $V_{SF}$ , for  $\Delta m^2 = (4 - 50)$  eV<sup>2</sup> the additional level crossings appear in the region  $r \sim (30 - 100)$  km: second flavor crossings  $\nu_e - \nu_\tau$ , and second spin-flavor crossings  $\bar{\nu}_e - \nu_\tau$ . The order of resonances from the center is the following: spin-flavor (s), flavor (f), flavor (f), spin-flavor (s) —  $s, f, f, s$ . Note that now there is some part of the profile where the potential increases with distance, and consequently, the order of resonances is reversed: neutrino crosses first the flavor resonance and then the spin-flavor one. This may have important consequences for observations (see sect. 6.4).

At distances (30 - 100) km the adiabaticity bound for the spin-flip equals  $B_A = (1 - 2) \cdot 10^{11}$  Gauss. This is only slightly higher than that in the inner edge of the isotopically neutral region. However, the existence of such a field is more probable in the inner part; for the profile (2) with  $k = 2$  and  $B_0 = 10^{13}$  Gauss the field is only 2 - 3 times smaller than the adiabaticity bound. Thus the magnetic moment  $\mu \sim 10^{-12} \mu_B$  may give strong spin-flip effect here.

If in the inner part all four transitions are efficient, there is no observable effect: the final state will coincide with the initial one.

## 6 Implications

In principle, future experiments will give information on the energy spectra of different neutrino species. Confronting these spectra with each other, one can get essentially model independent



information about possible neutrino transitions. It is convenient to introduce three types of original spectra: soft,  $F_s(E)$ , middle,  $F_m(E)$ , and hard,  $F_h(E)$ , which coincide with original  $\nu_e$ -,  $\bar{\nu}_e$ -, and  $\nu_\mu$ -spectra, respectively. The muon and tau neutrinos and antineutrinos are indistinguishable in the standard electroweak model at low energies, and will be detected by neutral currents. Therefore we will consider the total flux of the “non electron neutrinos”,  $F(\nu_{ne})$ . If there is no neutrino transitions, then at the exit:

$$F(\nu_e) = F_s, \quad F(\bar{\nu}_e) = F_m, \quad F(\nu_{ne}) = 4F_h. \quad (29)$$

Let us find the signatures of the spin-flip transitions, as well as the sensitivity of the  $\nu$ -burst studies to the neutrino magnetic moments. We estimate the values of  $B$  (at  $\mu = 10^{-12}\mu_B$ ) needed for different effects to be observable.

### 6.1 Sensitivity to magnetic moments and magnetic fields

The suppression of the effective potential by 3 – 4 orders of magnitude diminishes the strength of the magnetic field (magnetic moment) needed for a strong spin-flip effect. The adiabatic and the precession bounds decrease by 1.5 – 2 and 3 – 4 orders of magnitude respectively. We take as the criterion of the sensitivity of the  $\nu$ -burst studies to the spin-flip effects the magnitude of the magnetic field strength  $B_s$  ( $\mu = 10^{-12}\mu_B$ ) at which the probability of transition is  $\sim 1/2$  at least for some neutrino energy interval. According to Fig. 2, in the most part of the isotopically neutral region ( $r \leq 0.3R_\odot$ ) the adiabaticity bound is below the precession bound. Only in the external part of star the precession could be more preferable. Consequently, for  $r \leq 0.3R_\odot$  the sensitivity limit corresponds to inequality  $2\mu B < V_{SF}$ . The latter means that mixing is small everywhere apart from the resonance layer and the transition is due to the level crossing with not so strong adiabaticity violation. The nonaveraged over the precession phase probability  $P \sim 1/2$ , can correspond to the value of the Landau-Zener probability  $P_{LZ} \sim 0.75$ . Therefore we will define the sensitivity limit  $B_s(r)$  in a given point as the strength of the magnetic field, for which  $P_{LZ}(r) \sim 0.75$ . According to the estimations in section 3.2, the sensitivity bound can be about 3 times smaller than the adiabaticity bound:  $B_s \approx B_A/3$  (fig. 3).

For the effect to be appreciable, the size of the region with magnetic field,  $\Delta r_B$ , should be comparable with the size of the resonance region. If  $V_{SF} \propto r^{-3}$ , we get  $\Delta r_B = (dV_{SF}/dr)^{-1}2\Delta V_R \approx 4\mu Br/3V_{SF}$ , and in particular, for  $2\mu B/V_{SF} < 0.3$ :  $\Delta r_B < 0.2r$ . In fact,  $B_s$  should be considered as the average field in the region  $\Delta r_B$ .

The transition takes place in the resonance region whose position depends via the resonance condition on  $E/\Delta m^2$ . Therefore for fixed  $E/\Delta m^2$  one can define the sensitivity limit  $B_s$  in a

certain region of star  $r = r(V_{SF}(E/\Delta m^2))$ . For  $\Delta m^2 = (0.3 - 1) \cdot 10^{-5} \text{ eV}^2$  ( $E \sim 20 \text{ MeV}$ ) which corresponds to the MSW solution to the solar neutrino problem [26, 27] the spin-flip resonance lies at  $r \sim (1 - 3) \cdot 10^{-2} R_\odot$ , and according to fig. 2, the sensitivity limit equals  $B_s = (2 - 5) \cdot 10^6$  Gauss. For the oscillation solution of the atmospheric neutrino problem ( $\Delta m^2 \sim 10^{-2} \text{ eV}^2$ ) [28] the resonance is at  $r \sim (2 - 3) \cdot 10^{-3} R_\odot$ , and  $B_s \sim 10^9$  Gauss.

In the external part of the isotopically neutral region,  $r = (0.3 - 0.7) R_\odot$ , the precession bound is essentially below the adiabaticity bound. However, here for  $2\mu B \sim V_{SF}$  the precession length is already comparable with the distance to the center of star and the condition (3) becomes more important. At  $r \approx 0.3 R_\odot$  one gets  $B_s \sim (2 - 3) \cdot 10^4$  Gauss. This region corresponds to values  $\Delta m^2 = (10^{-9} - 10^{-8}) \text{ eV}^2$  which are interesting from the point of view of the resonant spin-flip in the convection zone of the Sun.

In the range  $r \approx (0.7 - 1) R_\odot$  the matter effect can be neglected and the sensitivity is determined by vacuum precession:  $B_s > 2/R_\odot \sim (2 - 3) \cdot 10^4$  Gauss. This number can be compared with value of  $B$  needed to solve the solar neutrino problem. For strong  $\nu_{eL} \rightarrow \bar{\nu}_{\mu R}$  conversion in convection zone of the sun ( $r \sim (0.7 - 1) R_\odot$ ) one needs the magnetic field as large as  $B \approx 3 \cdot 10^5$  Gauss [29]. In supernova, at the same distance from the center, the field of about  $10^4$  Gauss is enough. Conversely, if the magnetic field is  $\sim 3 \cdot 10^5$  Gauss, the  $\nu$ -burst will be sensitive to  $\mu \sim 3 \cdot 10^{-14} \mu_B$ .

Note that in the isotopically neutral region one needs for appreciable  $\nu_{eL} - \bar{\nu}_{\mu R}$  conversion 1.5 - 2 orders of magnitude smaller field than for conversion into a sterile state:  $\nu_{eL} \rightarrow \nu_{sR}$ .

Comparing the above results with those of sect. 5.3 we find that the sensitivity to  $\mu$  can be even higher in the isotopically neutral region than possible sensitivity to  $\mu$  in the central region of star. (Of course, the latter corresponds to large values of  $\Delta m^2$ ).

## 6.2 Bounds on $\mu B$ from SN1987A

The spin-flip  $\nu_\mu \rightarrow \bar{\nu}_e$  leads to an appearance of the high energy tail in the  $\bar{\nu}_e$ -spectrum at the Earth:

$$F(\bar{\nu}_e) = (1 - P_s)F_m + P_s F_h, \quad (30)$$

where  $P_s$  is the transition probability. At small mixing angles the flavor conversion does not change this result (see fig. 3). Note that in (30)  $P_s$  can be close to 1, in contrast with averaged vacuum oscillation effect which gives  $P \leq 1/2$ .

The absence of the distortion of the  $\bar{\nu}_e$ -energy spectrum, and in particular, the absence of the high energy tail, gives the bound on  $\mu B$  as function of  $\Delta m^2$ . For a class of supernovae models the data from SN1987A allow to get the restriction  $P_s < 0.35$  under the assumption that  $P_s$  does not depend on energy [32]. In fact, at the border of sensitivity the suppression pit is rather

thin (figs. 5, 6) and the energy dependence can not be completely neglected. In this case the strongest observable effect takes place, when a position of the pit coincides with the high energy part of the  $\nu_\mu$ -spectrum. The sensitivity limit obtained in sect. 6.1 gives an estimation of the upper bound on  $\mu B(r)$ . The value of the potential  $V_{SF}(r)$  in the corresponding point  $r$  determines via the resonance condition the value of  $\Delta m^2$ . For example, at  $\Delta m^2 \simeq 10^{-8}$  eV<sup>2</sup> (resonance at  $r = 0.3R_\odot$ ) one gets the upper bound as  $B(0.3R_\odot) < 2 \cdot 10^4$  Gauss. Similarly, if  $\Delta m^2 = 10^{-6}$  eV<sup>2</sup>:  $B(0.1R_\odot) < 3 \cdot 10^5$  Gauss, and if  $\Delta m^2 \sim 3 \cdot 10^{-5}$  eV<sup>2</sup>:  $B(0.01R_\odot) < 10^7$  Gauss etc.. In the case of the global magnetic field (2) with  $k = 2$  these bounds correspond to the bound on the field at the surface of the protonneutron star  $B_0 \lesssim 10^{13}$  Gauss ( $\mu = 10^{-12} \mu_B$ ).

### 6.3 Transitions of the degenerate or massless neutrinos

The mass differences  $\Delta m^2 \lesssim 10^{-10}$  eV<sup>2</sup> can be neglected for the neutrino energies  $E \sim 5 - 50$  MeV. This corresponds to the asymptotic region in  $P$ -dependence on  $E/\Delta m^2$  (fig. 4, 5). As we have noticed in sect. 2, for  $\Delta m^2 \approx 0$  there are two level crossings  $\nu_e - \bar{\nu}_\mu$  and  $\bar{\nu}_e - \nu_\mu$  at the same point,  $r \sim R_\odot$ . The crossings are induced by change of the nuclear composition on the border between the H-envelope and the <sup>4</sup>He-layer. However, in this region the effective density changes very quickly, and the adiabaticity condition implies very strong magnetic field  $B((0.7 - 1)R_\odot) > 3 \cdot 10^5$  Gauss which exceeds the precession bound. The effect is mainly due to the precession, and the field should be as strong as  $B \sim (2 - 5) \cdot 10^4$  Gauss. The probabilities of transitions  $\nu_e \leftrightarrow \bar{\nu}_\mu$  and  $\bar{\nu}_e \leftrightarrow \nu_\mu$  are equal and do not depend on energy. The final spectra of  $\nu_e$  and  $\bar{\nu}_e$  equal:  $F(\nu_e) = (1 - P_s)F_s + P_sF_h$ ,  $F(\bar{\nu}_e) = (1 - P_s)F_m + P_sF_h$ . In the case of complete transformation,  $P_s \approx 1$ , the  $\bar{\nu}_e$ - and  $\nu_e$ - energy spectra coincide with the initial  $\nu_\mu(\bar{\nu}_\mu)$ -spectrum:

$$F(\nu_e) = F(\bar{\nu}_e) = F_h \quad (31)$$

For  $\Delta m^2 > (10^{-9} - 10^{-8})$  eV<sup>2</sup> (which is interesting for the spin-flip of solar neutrinos [33]) the effect of the mass splitting becomes important. The probabilities of  $\bar{\nu}_e \rightarrow \nu_\mu$  and  $\nu_e \rightarrow \bar{\nu}_\mu$  transitions are different, and depend on energy.

### 6.4 Distortion of neutrino energy spectra

Using the matrix of the transition probabilities for the isotopically neutral region (27) and the initial conditions (28) we get for the final neutrino spectra:

$$\begin{aligned} F(\bar{\nu}_e) &= (1 - P_s)(1 - P'_s)F_m + [(1 - P_s)P'_s + P_s]F_h , \\ F(\nu_e) &= (1 - P_f)(1 - P'_f)F_s + [P'_fP'_s(1 - P_f) + P_fP_s(1 - P'_s)]F_m \end{aligned}$$

$$\begin{aligned}
& + [(1 - P_f)P'_f(1 - P'_s) + P_f(P_sP'_s + 1 - P_s)]F_h , \\
F(\nu_{ne}) & = a_s F_s + a_m F_m + a_h F_h ,
\end{aligned} \tag{32}$$

where

$$\begin{aligned}
a_s & = P'_f + P_f(1 - P'_f) \\
a_m & = P_f P'_f P'_s + (1 - P'_f)P'_s + (1 - P_f)P_s(1 - P'_s) \\
a_h & = 4 - a_s - a_m.
\end{aligned} \tag{33}$$

The important conclusions can be drawn from (32, 33) immediately. The  $\bar{\nu}_e$ -spectrum is a mixture of the middle (the original  $\bar{\nu}_e$  - spectrum) and hard components. It does not acquire soft component, except for the case of the non-monotonous change of the density in the central part of the star (see latter). The spectrum depends on the spin-flip probabilities  $P_s$  and  $P'_s$  and does not depend on probabilities of the flavor transitions. The changes are stipulated by the spin-flip effects only. Thus the distortion of the  $\bar{\nu}_e$  - spectrum, and in particular, the appearance of the hard component can be considered as the signature of the spin-flavor conversion.

According to fig. 8, the spin-flip may result in a variety of distortions of the  $\bar{\nu}_e$ -spectrum. In particular, when the transition probability  $P_s$  is constant, the permutation of the  $\bar{\nu}_e$ - and  $\nu_\mu$ -spectra can be symmetric, so that  $F(\bar{\nu}_e) \simeq (1 - P_s)F_m + P_s F_h$ , Such an effect is realized if the spectra are in the asymptotic region of the suppression pit or in the region of strong (complete) transformation. The transition can be asymmetric, so that in  $\bar{\nu}_e$ -spectrum the suppression of the  $F_m$ -component is weaker than the appearance of  $F_h$ -component and vice versa. This is realized, when the spectra are at the edges of the suppression pit or in the modulated resonance region. Note that the typical energy scale of the modulations of the probability can be characterized by factor 2 - 3. Therefore the spin-flavor transition results in a smooth distortion of each component. The fine structure of the energy spectrum ( $\Delta E \sim 1 - 2$  MeV) can be due to the jumps of density or/and the field twist in the inner parts of the star (see sect. 7).

Two remarks are in order. The change of the  $\bar{\nu}_e$ -spectrum is expected also if flavor mixing is large. In this case, however, one gets an energy independent interchange of the spectra with the transition probability  $P < 0.5$ . If the neutrino mass hierarchy is inverse, the properties of the transitions in the neutrino and antineutrino channels should be interchanged. In particular,  $\bar{\nu}_e$ -spectrum will acquire the soft component.

According to (33), the final  $\nu_e$ -spectrum is, in general, an energy dependent combination of all three original spectra. However,  $F_m$  component appears only if there are both spin-flavor and flavor transitions. Also the spin-flavor transition results in appearance of the  $F_m$  component in final  $\nu_\mu$ -spectrum.

#	$F(\nu_e)$	$F(\bar{\nu}_e)$	$F(\nu_{ne})$	transitions
1	$F_s$	$F_m$	$4F_h$	no transitions
2	$F_h$	$F_m$	$3F_h + F_s$	$f; f'; f'f$
3	$F_s$	$F_h$	$3F_h + F_m$	$s; s'; s's$
4	$F_m$	$F_h$	$3F_h + F_s$	$sf; s'f'; f'sf; s'f's$
5	$F_h$	$F_h$	$2F_h + F_s + F_m$	$s'f; f's; s'fs; f's'f; f's'fs$

Table 1: The final neutrino spectra in the case when transitions are either complete or completely inefficient:  $P_i \approx 0$  or 1. In the fifth column we give a list of the transitions which result in a given final spectrum. Here  $f$  and  $f'$  denote the flavor transitions  $\nu_e - \nu_\mu$  and  $\nu_e - \nu_\tau$ ,  $s$  and  $s'$  denote the spin-flip transitions  $\bar{\nu}_e - \nu_\mu$  and  $\bar{\nu}_e - \nu_\tau$ , respectively;  $sf$  denotes a combination of the two complete transitions: first  $\bar{\nu}_e - \nu_\mu$  and then  $\nu_e - \nu_\mu$  etc.

The modifications of the spectra are especially simple, when the resonant transitions are either completely efficient or completely inefficient:  $P_i = 0$  or 1 [17]. In this case a complete permutation of the original spectra occur. Moreover, as follows from (33, 34), there are only four possible types of final spectra (Table I).

According to the Table I, the flavor transitions (# 2) result in a hard  $\nu_e$ -spectrum, whereas  $\bar{\nu}_e$ -spectrum is unchanged. Correspondingly, the  $\nu_{ne}$ -flux acquires a soft component. The neutronization peak consists of  $\nu_{ne}$ -neutrinos. The spin-flavor conversion only (# 3) leads to a hard  $\bar{\nu}_e$ -spectrum and to unchanged  $\nu_e$ -spectrum. The flavor conversion in the inner part of star could be efficient during the early stage of the burst, so that the spectra #3 for cooling stage can be accompanied by the  $\nu_{ne}$ -neutronization peak. The spin-flavor and the subsequent flavor transitions of  $\bar{\nu}_e$  in the inner or outer parts of the star result in the  $\nu_e$ -spectrum coinciding with the initial  $\bar{\nu}_e$ -spectrum,  $F_m$  (# 4). In this case  $\bar{\nu}_e$  has hard spectrum  $F_h$ . The same final spectra (# 4) appear also if in addition some other transitions take place which do not influence the neutrino flux originally produced as  $\bar{\nu}_e$ . The flavor transition of  $\nu_e$  and the spin-flavor transition of  $\bar{\nu}_e$  result in the same hard spectra for  $\nu_e$  and  $\bar{\nu}_e$  (#5). In principle, future experiments will be able to distinguish these possibilities.

If the transitions are incomplete, the final spectra are certain energy dependent combinations of the above five spectra.

The spectra can show a strong time dependence. The original spectra themselves depend on time: the temperatures decrease, and moreover, they decrease differently for different neutrino species. Also the transition probabilities change with time due to the variations of the effective potential profile in the inner part.

Interesting effect can be related to the existence of a region in which the density increases with distance. As we have noticed, here the order of resonances is changed: neutrinos first cross the flavor resonance and then the spin-flavor resonance. In this case  $\nu_e$  can be transformed into  $\bar{\nu}_e$ ; the final  $\bar{\nu}_e$ -spectrum will contain the soft component, and moreover the neutronization peak will consist of  $\bar{\nu}_e$ . Such a modification of spectra can be realized, if two inner resonances  $s$  and  $f$ , are inefficient. They are at the surface of the protoneutron star, where the density is changed very quickly, and therefore the adiabaticity could be strongly broken.

## 7 Effects of magnetic field twist

### 7.1 Field twist. Scale of twist

If the direction of the magnetic strength lines changes with distance, the propagating neutrinos feel the rotation (twist) of the magnetic field. The field twist leads to the splitting of the levels with different helicities by the value  $\dot{\phi}$  (see (15)) [30]. The effect can be considered as the modification of the effective potential:

$$V_{SF} \rightarrow V_{\phi} = V_{SF} + \dot{\phi}. \quad (34)$$

Thus the field twist changes the level crossing picture (the positions of resonances). However, since the flavor and spin-flavor resonances are strongly separated due to the isotopical neutrality of the medium, the shift (34) hardly induces the spatial permutation of resonances [30].

The field twist can be characterized by the scale of twist,  $r_{\phi}$ :

$$r_{\phi} \equiv \frac{\pi}{\dot{\phi}}, \quad (35)$$

so that on the way,  $r_{\phi}$ , the total rotation angle (in case of uniform rotation) equals  $\Delta\phi = \pi$ .

It is natural to suggest that the total rotation angle is restricted by

$$\Delta\phi \leq \pi. \quad (36)$$

For example, the twist appears, when the neutrinos cross the toroidal magnetic field with strength lines winding around the torus. In this case the maximal rotation angle is  $\pi$ , i.e. the bound (36) is fulfilled. Let  $\Delta r_B$  be the size of the region with the magnetic field, then  $\Delta\phi \sim \dot{\phi}\Delta r_B$ , and the condition (36) implies

$$r_{\phi} \gtrsim \Delta r_B. \quad (37)$$

That is the scale of the rotation is comparable or larger than the region with the magnetic field. For the global field one has  $\Delta r_B \sim r$ , and therefore

$$r_{\phi} \geq (0.1 - 1)r. \quad (38)$$

As we will see the bound on the total rotation angle (36) restricts strongly the effects of the field twist.

## 7.2 Effect of density suppression

Let us consider possible increase of sensitivity to  $(\mu B)$  due to the field twist. According to (34) at  $\dot{\phi} = \dot{\phi}_c$ , where

$$\dot{\phi}_c = -V_{SF}(r), \quad (39)$$

the matter effect is completely compensated at the point  $r$ . Let us define the critical rotation scale,  $r_\phi^c$ , at which the condition (39) is fulfilled:

$$r_\phi^c = -\frac{\pi}{V_{SF}}. \quad (40)$$

(Note that  $r_\phi^c$  coincides up to the factor 2 with the refraction length). At  $r_\phi \sim r_\phi^c$  the effect of field twist can be essential, and for  $r_\phi < r_\phi^c$ , it even dominates over the density effect. Comparing  $r_\phi^c$  with the distance from the center,  $r$ , we find (fig. 9) that  $r_\phi^c/r \geq 1$  for  $r \geq 5 \cdot 10^{-2} R_\odot$ , and  $r_\phi^c \ll r$  for  $r < 5 \cdot 10^{-3} R_\odot$ . In the inner parts of the star the critical scale is much smaller than the distance from center, e.g., at  $r = 10^{-3} R_\odot$  one gets  $r_\phi \simeq 20$  cm. The condition (38) is fulfilled for  $r \simeq 5 \cdot 10^{-3} R_\odot$ . Let us stress that the isotopical neutrality essentially enlarges the region, where (38) is satisfied and therefore the field twist can be important.

Suppose the equality (39) is fulfilled in some layer of size  $\Delta r$  (evidently, the field twist should be nonuniform). In  $\Delta r$  the spin-flip effect has a character of precession with maximal depth, and the sensitivity to  $\mu B$  is maximal. Let us estimate  $\mu B$  taking into account the restriction (36). The total rotation angle  $\Delta\phi$  equals

$$\Delta\phi = \int_{\Delta r} \dot{\phi}(r) dr = - \int_{\Delta r} V_{SF}(r) dr, \quad (41)$$

and if  $\Delta r \ll r$ :

$$\Delta\phi \sim -V_{SF} \Delta r. \quad (42)$$

The spin-flip probability is of the order one, when  $\Delta r \simeq \pi(2\mu B)^{-1}$ . Substituting this  $\Delta r$  in (42), we get the relation:

$$\mu B \approx \frac{\pi V_{SF}}{2\Delta\phi}. \quad (43)$$

Finally, (43) and the bound on the total angle of the twist (36) give  $\mu B > V_{SF}/2$  which precisely coincides with the precession bound (6). Thus, the field twist can relax the precession bound by factor 1/2 at most, and to the further increase of the sensitivity one should admit the field rotation on the total angle which exceeds  $\pi$ .

In the external layers ( $r \geq 0.1R_\odot$ ),  $\Delta r$  is larger than  $r$ , and the compensation (39) implies fine tuned profiles of  $\dot{\phi}(r)$  and  $V(r)$  in a wide spatial region which seems rather unnatural. On the other hand, if the compensation takes place in the inner part ( $r < 0.1R_\odot$ ) then  $\Delta r \ll r$ . However, here the precession bound is more stringent than the adiabaticity bound, and the compensation does not allow to gain in the diminishing of the field strength. In the inner part the effect of the field twist can be due to influence on the adiabaticity.

### 7.3 Influence of field twist on the adiabaticity

Nonuniform field rotation ( $\ddot{\phi} \neq 0$ ) modifies the adiabaticity condition. The adiabaticity parameter equals:

$$\kappa_\phi = \frac{2(2\mu B)^2}{|\dot{V}_{SF} + \ddot{\phi}|}. \quad (44)$$

At

$$\ddot{\phi} \simeq -\dot{V}_{SF} \quad (45)$$

$\kappa_\phi \rightarrow \infty$ , i.e. there is a strong improvement of the adiabaticity. The field twist results in flattening of the potential, so that  $dV_\phi/dr \simeq 0$  or  $V_\phi \simeq \text{const.}$ , in some region  $\Delta r$ . Let us estimate the minimal value of the total rotation angle in this region. For this we suggest that  $\dot{\phi} = 0$  at the one of the edges of  $\Delta r$ . Then from (45), it follows that  $\Delta\phi \approx \dot{V}_{SF}(\Delta r)^2/2$ . Inserting  $\Delta r \approx \pi(2\mu B)^{-1}$  (the condition for the strong precession effect) in the last expression, we get

$$\Delta\phi \approx \frac{\pi^2 \dot{V}_{SF}}{2(2\mu B)^2} \sim \frac{\pi}{\kappa_R}, \quad (46)$$

i.e. the total rotation angle is the inverse value of the adiabaticity parameter without field twist. Therefore, if the adiabaticity is strongly broken,  $\kappa_R \ll 1$ , one needs  $\Delta\phi \gg \pi$  to get an appreciable spin-flip effect. For restricted values of total rotation angle (36) only weakly broken adiabaticity can be restored. The relation (46) means that if the transition without field twist is weak ( $\kappa \ll 1$ ), then field twist will induce a weak effect for  $\Delta\phi < \pi$ . On the other hand, if the transition without twist is strong ( $\kappa_R \sim 1$ ), then the field twist can make it even stronger but the absolute change of probability turns out to be always small (fig. 11).

The effect of the adiabaticity restoration due to field twist can be considered as the effect of precession in the region  $\Delta r$  with flat potential ( $V_\phi = \text{const.}$ ). For constant  $B$  (which we suggest for simplicity) the transition probability equals

$$P_s = \frac{(2\mu B)^2}{(2\mu B)^2 + (V_\phi - \frac{\Delta m^2}{2E})^2} \cdot \sin^2 \sqrt{(2\mu B)^2 + \left(V_\phi - \frac{\Delta m^2}{2E}\right)^2} \frac{\Delta r}{2}. \quad (47)$$



One can find from (47) that field twist leads to the distortion of the energy dependence of the probability in some energy interval  $\Delta E$  located at  $E/\Delta m^2 \simeq (2V_\phi)^{-1}$ . Let us estimate the size of  $\Delta E$ . According to (47)  $\Delta E$  is determined by the resonance width  $\Delta E/E \sim 4\mu B/V_{SF}$ . In turn,  $2\mu B$  can be estimated from (46) and the condition  $\Delta\phi < \pi$ :  $2\mu B \gtrsim \sqrt{(\pi\dot{V}_{SF})/2}$ . So that finally, we get

$$\frac{\Delta E}{E} \gtrsim \frac{\sqrt{2\pi\dot{V}_{SF}}}{V_{SF}} = \sqrt{\frac{2\pi}{H_{SF}V_{SF}}} \quad (48)$$

If  $V_{SF} \propto r^{-3}$  and  $H_{SF} \propto r$ , the relation (48) gives  $\frac{\Delta E}{E} \propto r$ . The closer the region with field twist to the center of the star the thinner the peak. For  $r \sim 10^{-2}R_\odot$ , one gets  $\frac{\Delta E}{E} \gtrsim 0.3$ . In external region of star ( $r > 0.1R_\odot$ ), the field twist results in smooth change of the probability in a wide energy region, and it is impossible to distinguish it from other effects (fig. 11). In any case the absolute value of  $\Delta P$  is small, unless  $\Delta\phi \gg \pi$ .

As follows from (44) the field twist can also destroy the adiabaticity, when  $|\ddot{\phi}| \gg |\dot{V}|$ . Randomly twisting field inhibit the conversion in such a way. This can result in bumps of the survival probability that may be similar to those due to density jumps.

## 8 Conclusion

1. For neutrino mass squared differences  $\Delta m^2 < 10 \text{ eV}^2$  (which are interesting for the cosmology, as well as for the physics of solar and atmospheric neutrinos) the resonant spin-flavor transitions ( $\nu_e \rightarrow \bar{\nu}_\mu$  etc.) take place in almost isotopically neutral region of collapsing star. In this region which extends from  $\sim 10^{-3}R_\odot$  to  $\sim R_\odot$  the deviation from the isotopical neutrality,  $2Y_e - 1$ , can be as small as  $10^{-3} - 10^{-4}$ . Correspondingly, the matter potential for the spin-flavor transitions, being proportional to  $(2Y_e - 1)$ , turns out to be suppressed by 3 - 4 orders of magnitude. Moreover, the potential changes the sign at the inner edge of the hydrogen envelope.

2. The suppression of the effective potential in the isotopically neutral region diminishes the values of  $(\mu B)$  needed to induce an appreciable spin-flip effects by 1.5 - 2 orders of magnitude. Thus, the sensitivity of the neutrino burst studies to the transition magnetic moments of neutrinos increases, being of the order  $10^{-13}\mu_B$  for  $\Delta m^2 = (10^{-8} - 10^{-1}) \text{ eV}^2$  and for a reasonable strength of the magnetic field. In particular, for  $\Delta m^2 = (10^{-8} - 10^{-9}) \text{ eV}^2$  the desired values of  $(\mu B)$  turn out to be 1.5 - 2 orders of magnitude smaller than those for a strong conversion of the solar neutrinos.

3. In the isotopically neutral region the potential changes very quickly in the layers with local ignition (jumps of the potential). The jumps result in distortion of the energy dependence of

probabilities. In particular, one can expect the appearance of thin peaks in the survival probability if the jump is situated in the inner part of the star.

4. Depending on the values of the neutrino parameters as well as on the magnetic field profile one expects a variety of the modifications of the neutrino spectra. In the case of a direct mass hierarchy and a small flavor mixing the main signature of the spin-flip effect is the distortion of the  $\bar{\nu}_e$ -energy spectrum, and especially the appearance of the high energy tail. In general, the final  $\bar{\nu}_e$ -spectrum is the energy dependent combination of the original  $\bar{\nu}_e$ -spectrum and the hard spectrum of the non-electron neutrinos. Another important signature of the spin - flip can be obtained from the comparison of the spectra of different neutrino species. In particular, the  $\bar{\nu}_e$ - and  $\nu_\mu$ -spectra can be completely permuted. The combination of the spin-flip effect with other (flavor) transitions may result in rather peculiar final spectra. For example,  $\nu_e$  may have the spectrum of the original  $\bar{\nu}_e$ , whereas  $\bar{\nu}_e$  may have the original  $\nu_\mu$ -spectrum. The electron neutrino and antineutrino spectra can be the same and coincide with the hard spectrum of the original muon neutrinos, etc.

5. The resonant spin-flip effect for the massless or the degenerate ( $\Delta m^2 \lesssim 10^{-10} \text{ eV}^2$ ) neutrinos can be induced by the change of the nuclear composition. Such a transition takes place both for neutrinos and antineutrinos in the same spatial region (near to the bottom of the H-envelope), resulting again in hard and equal  $\nu_e$ - and  $\bar{\nu}_e$ -spectra.

6. The absence of the considered effects allows one to get the bound on  $(\mu B(r))$  as a function of  $\Delta m^2$ . We estimate such a bound for SN 1987A.

7. In the isotopically neutral region, where the matter potential is strongly suppressed, the effects of (even) small field twist may be important. Field twist can further suppress the potential, thus increasing the sensitivity to the magnetic moment. However, if the total rotation angle is restricted ( $< \pi$ ), a possible diminishing of  $\mu B$  can be by factor 1/2 at most. The twist of the field may induce a distortion of the neutrino energy spectra. In particular, improving adiabaticity, in the inner part of the isotopically neutral region the field twist may lead to peaks of the transition probabilities.

## Acknowledgements

The authors are grateful to E. Kh. Akhmedov for discussions and for numerous remarks concerning this paper. H. A. would like to thank Prof. A. Salam, the International Atomic Energy Agency and UNESCO for hospitality at the International Centre for Theoretical Physics.

## References

- [1] S. Van den Bergh, Phys. Rep. **204**, 385 (1991).
- [2] K. Hirata et al., Phys. Rev. Lett. **58**, 1490 (1987).
- [3] R. M. Bionta et al., Phys. Rev. Lett. **58**, 1494 (1987).
- [4] E. N. Alexeyev et al., Phys. Lett. B **205**, 209 (1988).
- [5] M. Aglietta et al., Europhys. Lett. **3**, 1315 (1987).
- [6] C. Bari et al., Nucl. Inst. Meth. A **277**, 11 (1989); M. Aglietta et al., Nuov. Cim. A, **105** 1793 (1992).
- [7] Scientific and Technical Description of Mark II SNO Detector, ed. by E. W. Beier and D. Sinclair, Report SNO-89-15 (1989).
- [8] K. Nakamura, ICRR-Report-309-94-4.
- [9] P. Benetti et al., Nucl. Inst. & Meth. A315, 223 (1992), ibidem A332, 395 (1993).
- [10] D. B. Cline, preprint UCLA-CAA 107-3/94.
- [11] A. Cisneros, Astrophys. Space Sci. **10**, 87 (1970).
- [12] K. Fujikawa and R. E. Shrock, Phys. Rev. Lett. **45**, 963 (1980).
- [13] M. B. Voloshin, M. I. Vysotsky, and L. B. Okun, Zh. Eksp. Teor. Fiz. **91**, 754 (1986) [Sov. Phys. JETP **64**, 446 (1986)].
- [14] J. Schechter and J. W. F. Valle, Phys. Rev. D **24**, 1883 (1981); ibidem **25**, 283 (E) (1982).
- [15] C.-S. Lim and W. J. Marciano, Phys. Rev. D **37**, 1368 (1988).
- [16] E. Kh. Akhmedov, Sov. J. Nucl. Phys. **48**, 382 (1988); Phys. Lett. B **213**, 64 (1988).
- [17] E. Kh. Akhmedov and Z. G. Berezhiani, Nucl. Phys. B **373**, 479 (1992).
- [18] M. B. Voloshin, Phys. Lett. B **20**, 360 (1988).
- [19] J. T. Peltoniemi, Astron. & Astrophys., **254** 121 (1992).
- [20] E. Kh. Akhmedov, Sov. Phys. JETP **68**, 676 (1989).

- [21] M. Fukugita and S. Yazaki Phys. Rev. D **36**, 3817 (1987); G. G. Raffelt, Astrophys. J. **365**, 559 (1990); V. Castellani and S. Degl'Innocenti, Astrophys. J. **402**, 574 (1993).
- [22] M. Moretti, Phys. Lett. B **293**, 378 (1992).
- [23] S. E. Woosley and T. A. Weaver, Annu. Rev. Astron. Astrophys. **24**, 205 (1986).
- [24] S. E. Woosley, N. Langer and T. A. Weaver, Ap. J. **411**, 823 (1993).
- [25] P. I. Krastev and A. Yu. Smirnov, Mod. Phys. Lett. A **6**, 1001 (1991).
- [26] S. P. Mikheyev and A. Yu. Smirnov, Sov. J. Nucl. Phys. **42**, 913 (1985).
- [27] P. I. Krastev and A. Yu. Smirnov, Phys. Lett. B **338** 282 (1994).
- [28] R. Becker-Szendy et al., Phys. Rev. D **46**, 3720 (1992); Y. Fukuda et al., Phys. Lett. B **335**, 237 (1994).
- [29] see for latest discussion E. Kh. Akhmedov, A. Lanza and S. T. Petcov, SISSA Report 169/94/A-EP.
- [30] A. Yu. Smirnov, Phys. Lett. B **260**, 161 (1991); E. Kh. Akhmedov, S. T. Petcov, and A. Yu. Smirnov, Phys. Rev. D **48**, 2167 (1993).
- [31] A. Burrows, D. Klein and R. Gandhi, Phys. Rev. D **45**, 3361 (1992).
- [32] A. Yu. Smirnov, D. N. Spergel, and J. N. Bachall, Phys. Rev. D **49**, 1389 (1994).
- [33] E. Kh. Akhmedov, Phys. Lett. B **213**, 64 (1988).
- [34] L. B. Okun, Sov. J. Nucl. Phys., **48** 967 (1990); J. Pantaleone, Phys. Lett. B **287**, 128 (1992); S. Samuel, Phys. Rev. D **48**, 1462 (1993).

## Figure Captions

Figure 1. The dependence of the potentials for the spin-flavor conversion,  $\bar{\nu}_e \rightarrow \nu_\mu$ , (dotted and solid lines) and the flavor conversions,  $\nu_e \rightarrow \nu_\mu$ , (dashed line) on the distance from the center of the star ( $M = 15M_\odot$ ). At  $r \simeq 0.8R_\odot$ , the spin-flavor potential changes the sign, and for  $r > 0.8R_\odot$  we depict  $-V_{SF}$  which coincides with  $V_{SF}$  for  $\nu_e \rightarrow \bar{\nu}_\mu$  channel.

Figure 2. The qualitative dependence of the energy levels on the distance from the center of the star,  $r$ , for different values of  $\Delta m^2/2E$ . The energies are defined in such a way that  $H(\nu_e)(r) = 0$  (solid line). (The energy scale is relative). Dotted lines show a behaviour of the eigenvalues of the Hamiltonian near the crossing points. Also marked are the positions of the inner and outer edges of the isotopically neutral region. a).  $E/\Delta m^2 \approx 0$ ; b).  $E/\Delta m^2 \lesssim 3 \cdot 10^{-8} \text{ eV}^2$ ; c).  $E/\Delta m^2 \gtrsim 3 \cdot 10^{-8} \text{ eV}^2$ ;

Figure 3. The dependence of the adiabaticity  $B_A$  (solid line) and the precession  $B_P$  (dotted line) bounds for  $\mu_\nu = 10^{-12}\mu_B$  on the distance from the center of star. Also shown is the magnetic field profile (2) with  $B_0 = 1.5 \cdot 10^{13}$  Gauss and  $k = 2$  (dashed line).

Figure 4. Spatial picture of the ( $\bar{\nu}_e \rightarrow \nu_\mu$ )-spin-flavour transition. The dependence of the  $\bar{\nu}_e$ -survival probability on the distance from the center of the star for different strengths of the magnetic field. The field profile (2) was used with  $k = 2$  and  $B_0$  (in Gauss):  $5 \cdot 10^{12}$  (dashed-dotted line),  $1.5 \cdot 10^{13}$  (dashed line),  $5 \cdot 10^{13}$  (dotted line),  $1.5 \cdot 10^{14}$  (solid line). a).  $E/\Delta m^2 = 10^8 \text{ MeV/eV}^2$  b).  $E/\Delta m^2 = 10^6 \text{ MeV/eV}^2$ .

Figure 5. The  $\bar{\nu}_e$ -survival probability for the ( $\bar{\nu}_e \rightarrow \nu_\mu$ )-spin-flip transition in the global magnetic field as a function of  $E/\Delta m^2$  for different strengths of the magnetic field. The magnetic field profile (2) was used with  $k = 2$  and  $B_0$  (in Gauss):  $1.5 \cdot 10^{12}$  (bold solid line),  $5 \cdot 10^{12}$  (dashed line),  $1.5 \cdot 10^{13}$  (dashed-dotted line),  $5 \cdot 10^{13}$  (dotted line),  $1.5 \cdot 10^{14}$  (solid line).

Figure 6. The  $\bar{\nu}_e$ -survival probability for the ( $\bar{\nu}_e \rightarrow \nu_\mu$ ) - spin-flavor transition, in the local magnetic field as functions of  $E/\Delta m^2$  for different values of the magnetic field. A constant magnetic field  $B_c$  in the interval  $(1 - 3) \cdot 10^{-2}R_\odot$  was used.  $B_c$  (in Gauss):  $3 \cdot 10^7$  (solid line),  $6 \cdot 10^7$  (dashed line),  $2 \cdot 10^8$  (bold solid line),  $3 \cdot 10^8$  (dashed-dotted line).

Figure 7. The probabilities of different transitions for the neutrino system with a magnetic moment and a vacuum mixing as functions of  $E/\Delta m^2$ . The initial state is (a)  $\bar{\nu}_e$ , and (b)  $\nu_\mu$ . The lines show the probabilities to find in the final state  $\nu_e$  (solid),  $\bar{\nu}_e$  (dotted), and  $\nu_\mu$  (dashed line). A vacuum mixing angle  $\sin^2 2\theta = 10^{-2}$  and a constant magnetic field  $B_c = 10^4$  Gauss in the interval  $R = (0.1 - 1.3)R_\odot$  were used.

Figure 8. The distortion of the  $\bar{\nu}_e$ -spectrum. The dependence of the product (flux) $\times$ (energy squared) on energy for different sets of neutrino parameters and different configurations of the magnetic fields. The original  $\bar{\nu}_e$ -spectrum is shown by the bold solid line. The case of the complete  $\bar{\nu}_e - \nu_\mu$  transformation ( $F = F_h$ ) is shown by the solid line.

Figure 9. The critical scale of the field twist over the distance from the center of the star as a function of  $r$ .

Figure 10. The effects of the non-uniform field twist. The  $\bar{\nu}_e$ -survival probability of the spin-flip transition,  $\bar{\nu}_e \rightarrow \nu_\mu$ , as a function of  $E/\Delta m^2$  for different configurations (scales) of the field twist. The field profile (2) with  $k = 2$  and  $B_0 = 5 \cdot 10^{12}$  Gauss was used. The solid line shows the probability without field twist. The field twist is located in the region  $r_0 - (r_0 + \delta r)$ , and the profile of twist is described by  $\dot{\phi}(r) = (2\pi/\delta r)(1 - (r - r_0)/\delta r)$ ; the total rotation angle equals  $\pi$ . The curves correspond to  $r_0 = 5 \cdot 10^{-3}R_\odot$  and  $\delta r/R_\odot = 10^{-4}$  (dotted),  $5 \cdot 10^{-4}$  (dashed),  $2.5 \cdot 10^{-3}$  (dashed-dotted).

This figure "fig1-1.png" is available in "png" format from:

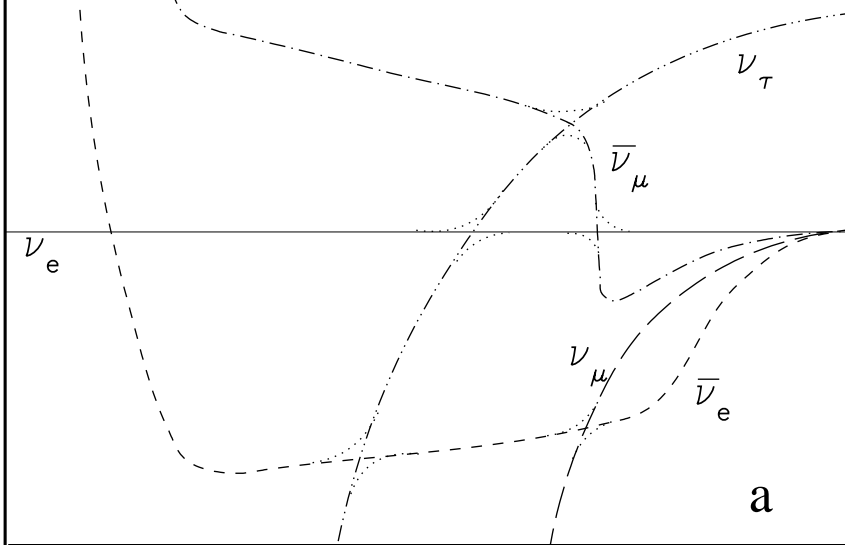
<http://arxiv.org/ps/hep-ph/9501283v1>

This figure "fig2-1.png" is available in "png" format from:

<http://arxiv.org/ps/hep-ph/9501283v1>

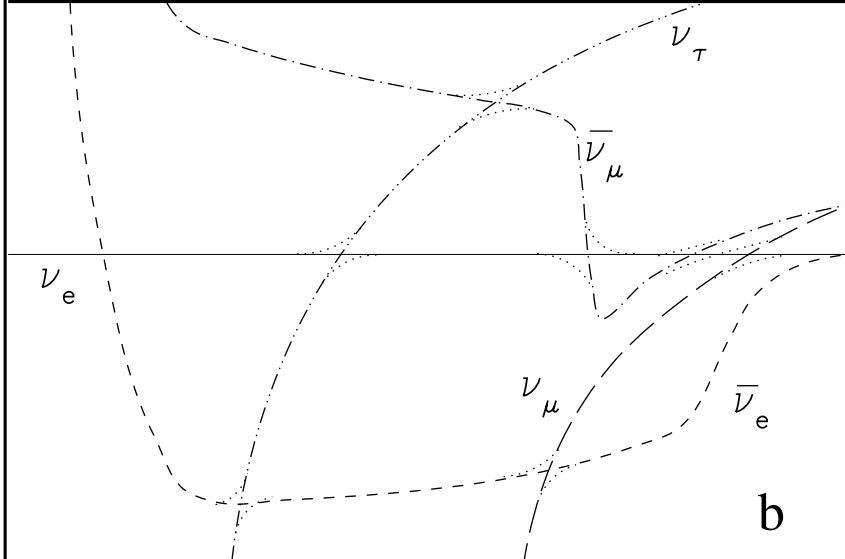


$H$



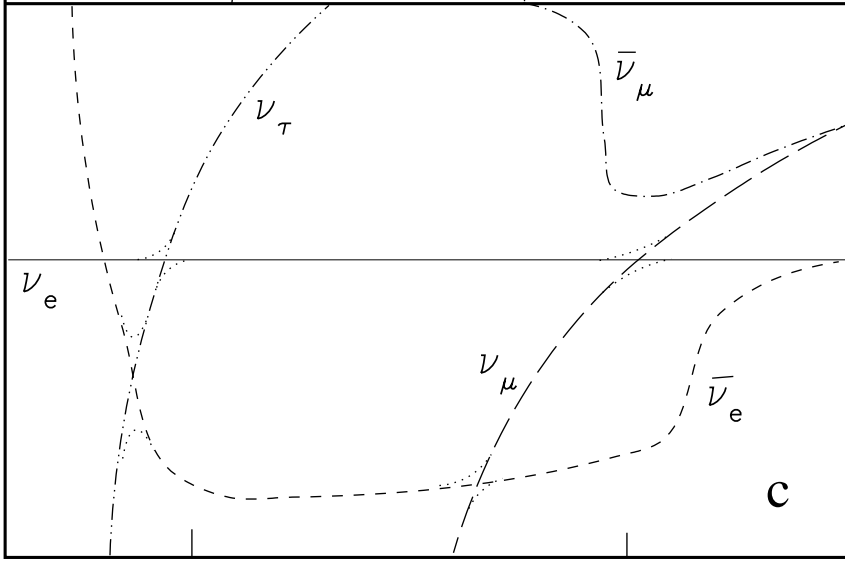
**a**

$H$



**b**

$H$



**c**

$r_{in}$

$r$

$r_{out}$

Fig 2

This figure "fig1-2.png" is available in "png" format from:

<http://arxiv.org/ps/hep-ph/9501283v1>

This figure "fig2-2.png" is available in "png" format from:

<http://arxiv.org/ps/hep-ph/9501283v1>

This figure "fig1-3.png" is available in "png" format from:

<http://arxiv.org/ps/hep-ph/9501283v1>

This figure "fig2-3.png" is available in "png" format from:

<http://arxiv.org/ps/hep-ph/9501283v1>

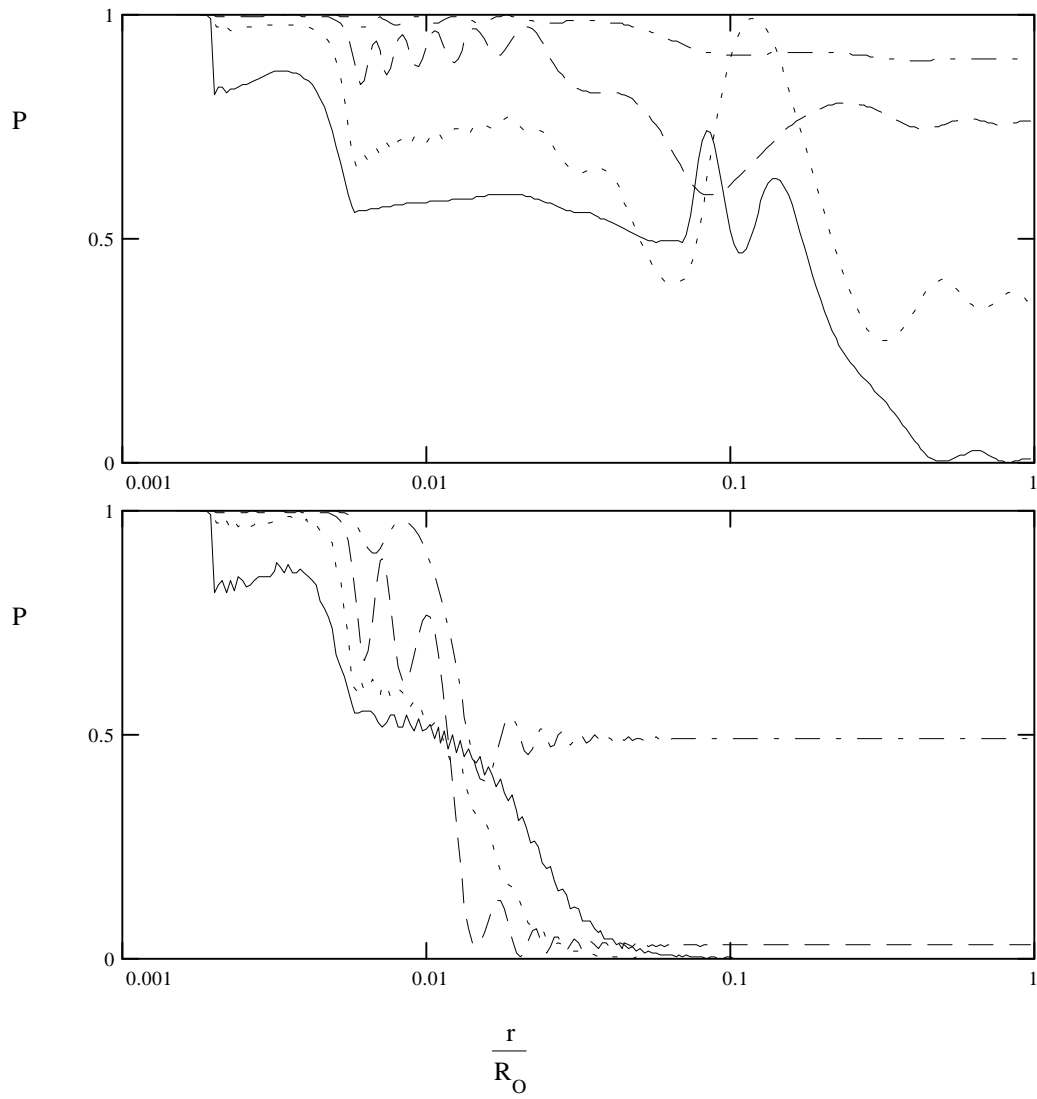


Fig 4

This figure "fig2-4.png" is available in "png" format from:

<http://arxiv.org/ps/hep-ph/9501283v1>

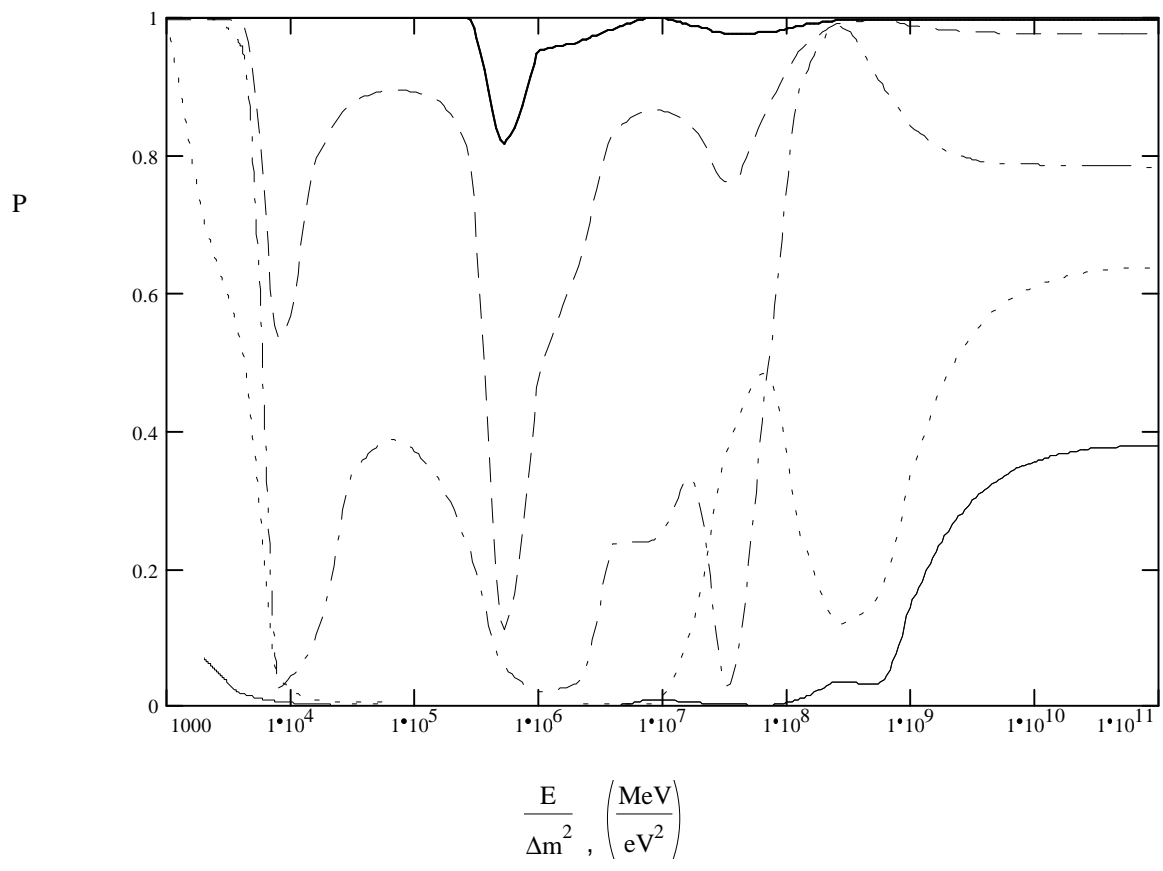


Fig 5



This figure "fig2-5.png" is available in "png" format from:

<http://arxiv.org/ps/hep-ph/9501283v1>

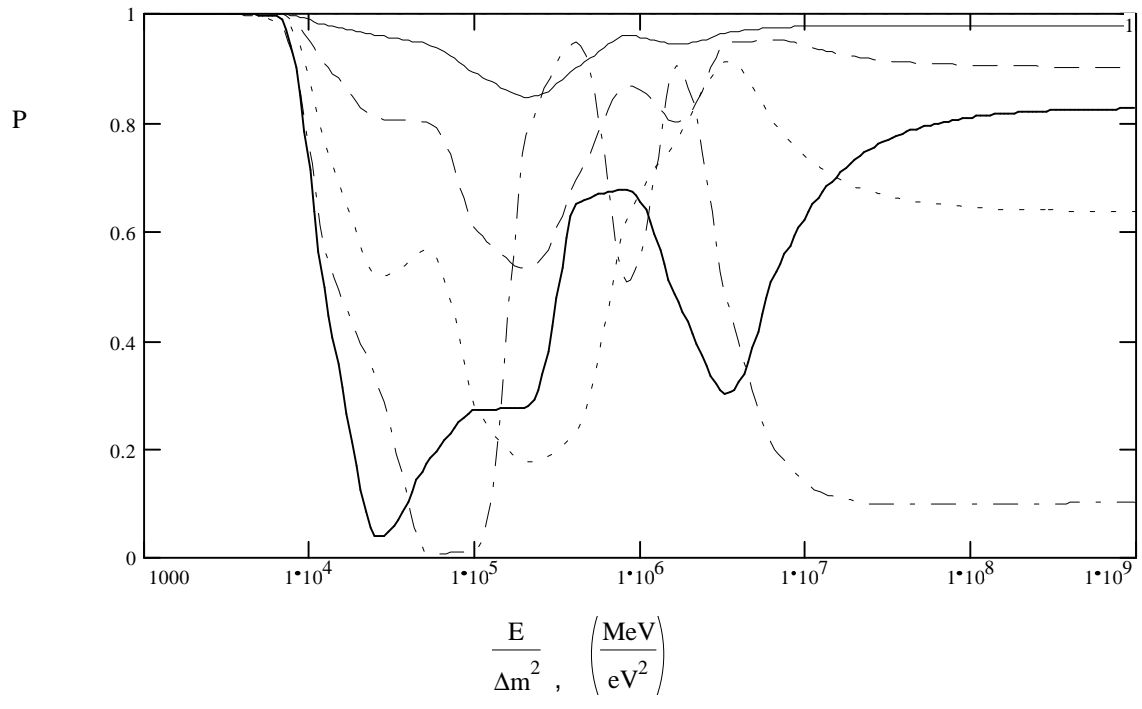


Fig 6

This figure "fig2-6.png" is available in "png" format from:

<http://arxiv.org/ps/hep-ph/9501283v1>

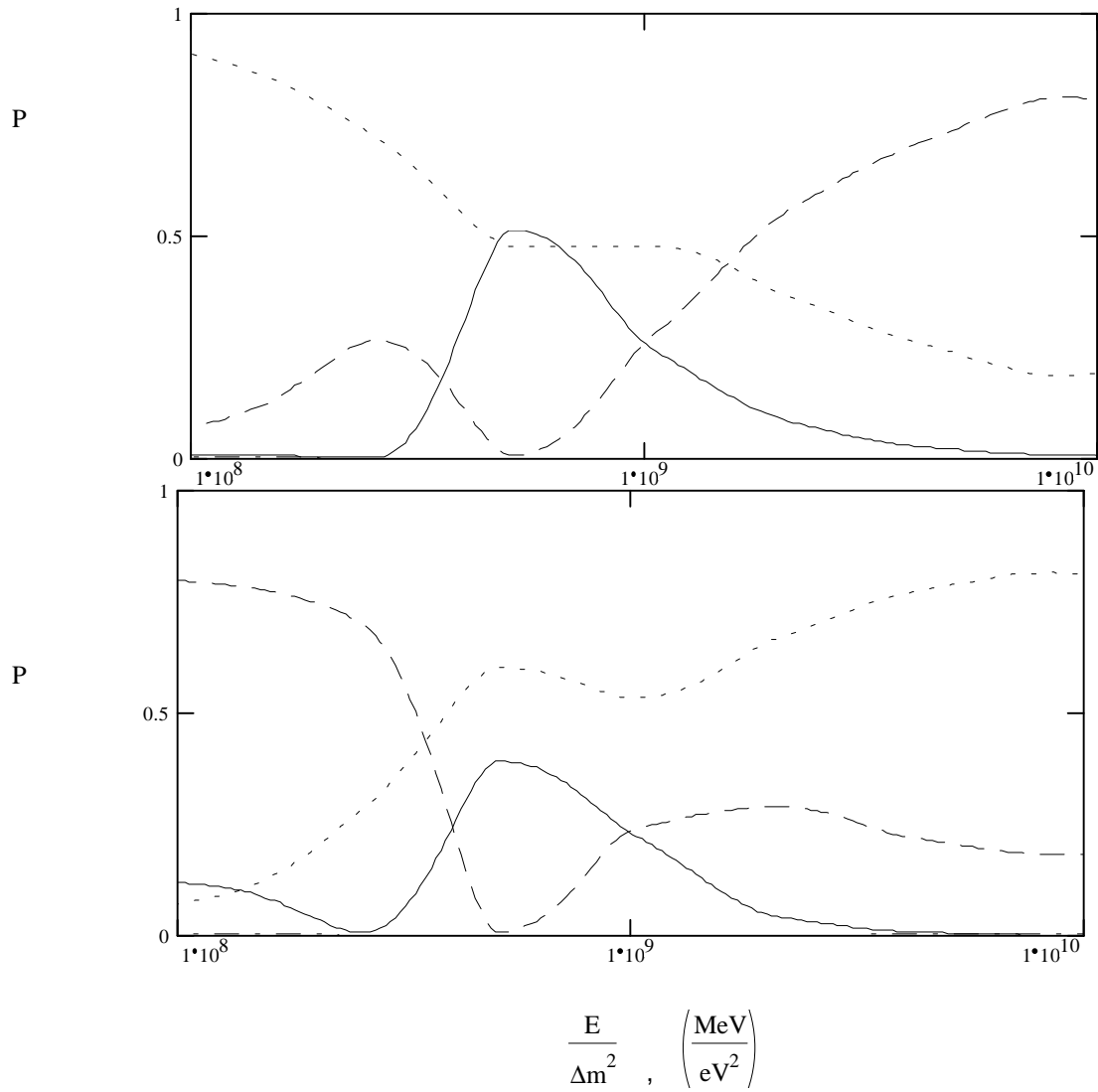


Fig 7

This figure "fig2-7.png" is available in "png" format from:

<http://arxiv.org/ps/hep-ph/9501283v1>

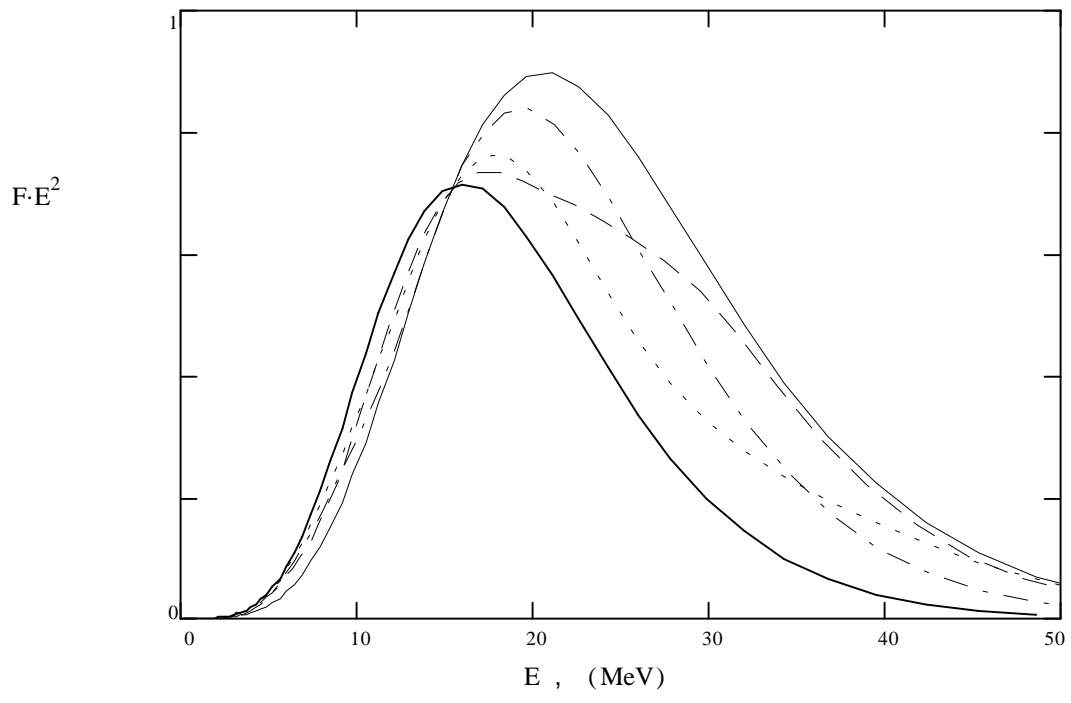


Fig 8

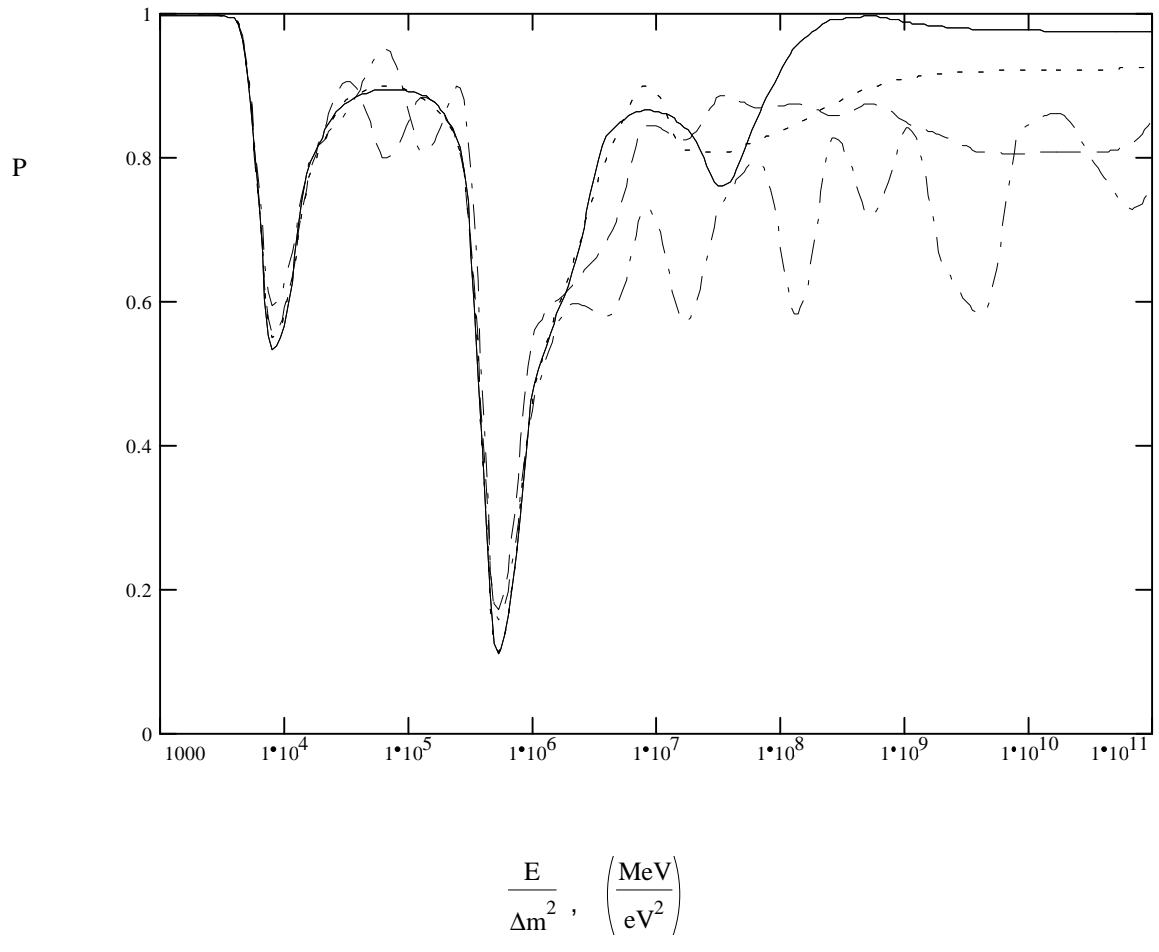


Fig 10

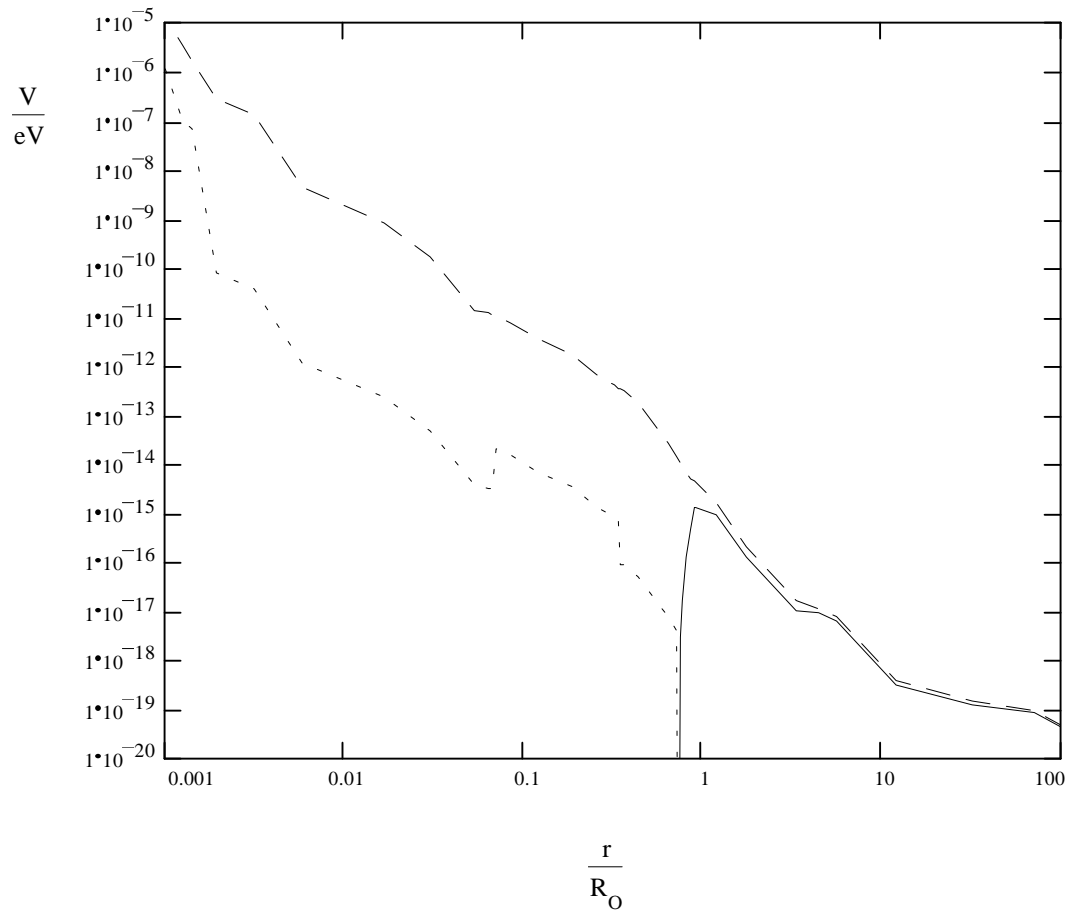


Fig 1



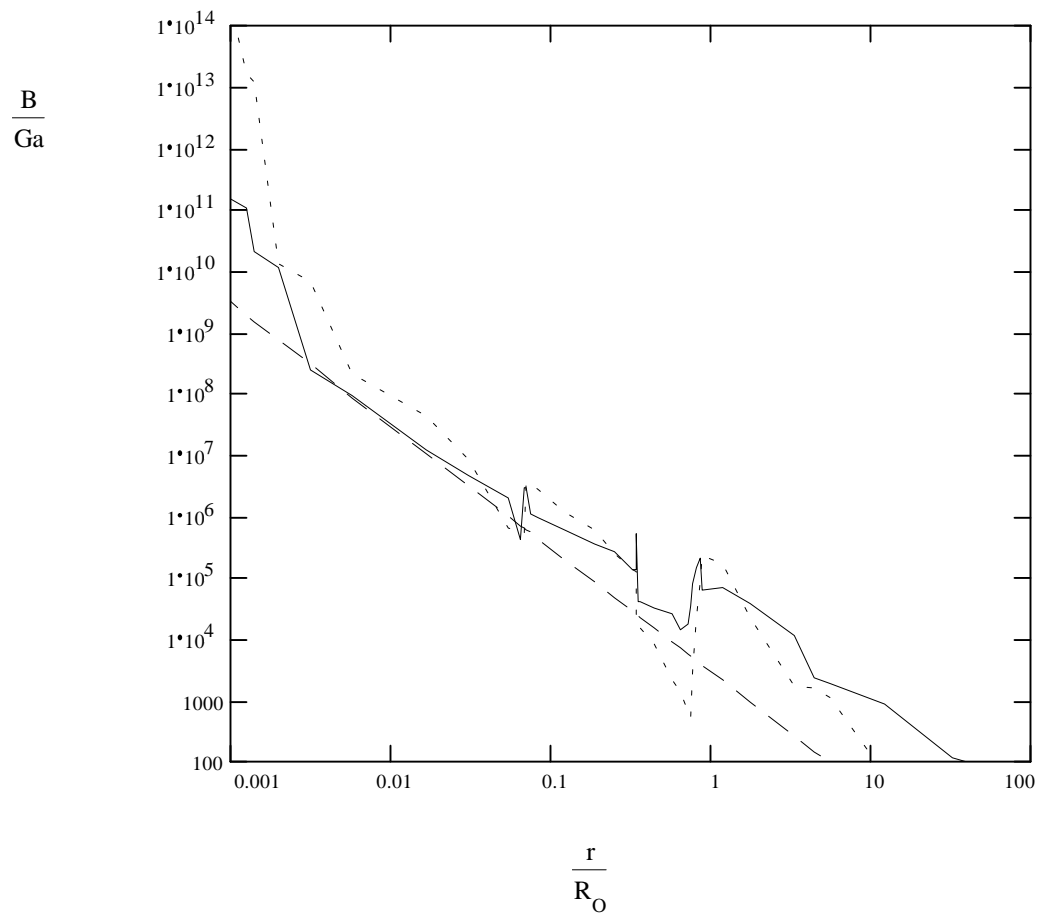


Fig. 3

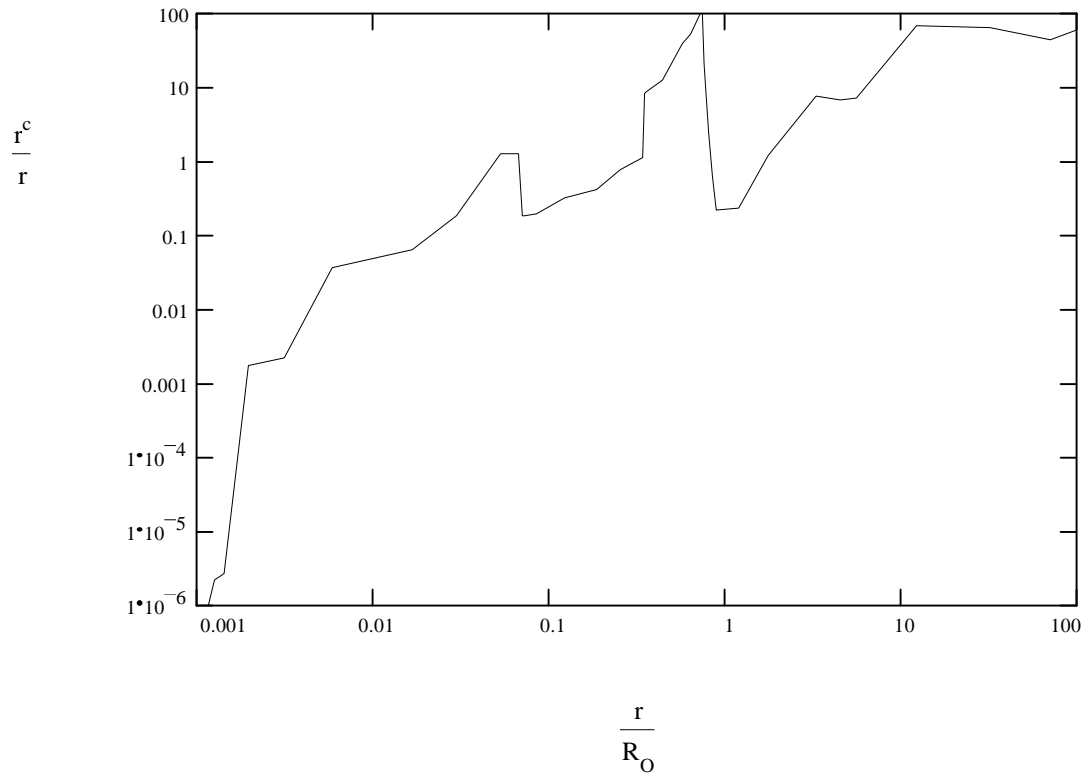


Fig 9